

# 11. Modulating-Anode Pulsers

The next family of pulse modulators is used with microwave tubes that have isolated, hollow anodes called modulating anodes (see Fig. 8-2). These pulsers must produce output voltages that are substantial percentages of the microwave-tube beam voltage—typically between 50% and 100%—but small intrapulse output current—typically only 0.1% of the total peak-beam current of the microwave tube. Electron guns for modulating anodes requiring pulse voltage in the 50% range are often referred to as “velocity-jump” guns because, even though the voltage between the modulating anode and the cathode determines the beam’s current density, the voltage between the cathode and beam tunnel (or grounded anode) determines the final electron velocity. The electrons, therefore, experience a “velocity-jump” in their passage between the modulating anode and beam tunnel.

The predominant load impedance on the modulating-anode pulser is the distributed capacitance, part of which derives from the capacitance within the electron gun between the modulating anode and the other electrodes, and the rest is associated with the pulse modulator itself, especially if it is of the “floating-deck” type. Modulators of this type have been built having a total load capacitance as high as 1 nF, although a typical value is less than half of that.

Microwave tubes with modulating anodes are designed to operate with voltage applied continuously to the cathode. Such tubes have operated with as much as 150 kV of cathode voltage, although recent technology has limited this figure, more or less, to 100 kV for reliable operation. This limitation, of course, still requires a pulse-modulator output-voltage capability of comparable magnitude.

## 11.1 Modulating-anode-pulsers topologies

### 11.1.1 *Passive pull-up, active pull-down*

The simplest of all modulator topologies is that shown in Fig. 11-1. It has a single active switch for pull-down, and it has a resistor,  $R$ , for passive pull-up. If the load (the electron gun and modulating anode) requires a full-voltage pulse, it is called a unity- $\mu$  modulating anode. In this case, the top of resistor  $R$  is simply connected to the high-voltage return bus. If adjustable output voltage over a range of operating pulse widths and repetition rates is required, an adjustable power supply is often used, as shown. This connection qualifies as the simplest because the deck containing the low-level electronics and the common for the switch-tube filament supply are both referenced to a nominally fixed voltage: the negative high voltage required by the microwave-tube electron-gun cathode. The common-mode rejection problem for the low-level drive signal is not as great as it will become in other topologies, as we shall see later.

This circuit arrangement has another modest advantage. The load capacitance contributed by the modulator itself is only the output capacitance of the switch tube, not the entire deck. The disadvantage, however, is usually a crush-

ing one: the off-deck switch tube is in the conducting state during the interpulse interval, which means that there is current flow in the pull-up resistor,  $R$ . The value of  $R$  determines the pulse rise time, which has the time-constant  $RC$ . For instance, if the load capacitance were 500 pF, which is not uncommon, and a time-constant of 10  $\mu$ s were desired,  $R$  would be  $10^{-5}$  seconds divided by  $5 \times 10^{-10}$  farads, or 20,000 ohms. If the microwave tube operated at 100 kV, the current through the resistor during the interpulse interval would be 100 kV/20,000 ohms, or 5 A. The peak dissipation would be 500 kW. If the duty factor was much less than 10%, the average dissipation would be 500 kW as well. If the pulse duty factor were considerably greater than 50%, this disadvantage would not be a problem. But such a high duty factor is rarely, if ever, the case. Moreover, if the adjustable-output power supply is used, this current must come from it. As rise time is sacrificed, dissipation is reduced, but it is obvious that much needs to be done to make this circuit practical.

### 11.1.2 Active pull-up, passive pull-down

For the reasons discussed above, the topology shown in Fig. 11-2 is considerably more popular. It also uses a single electronic switch as an active pull-up, with passive pull-down being provided by resistor  $R$ . But here, the output pulse is taken from the cathode of the switch tube rather than the anode, as was the case in Fig. 11-1. The switch tube is not a cathode follower, however. Its connection is often called a bootstrap circuit, in that the low-level grid-drive circuits are referenced to the switch-tube cathode, which is connected to an enclosure referred to as a "pulse deck," a "hot deck," or, most commonly, a "floating deck,"

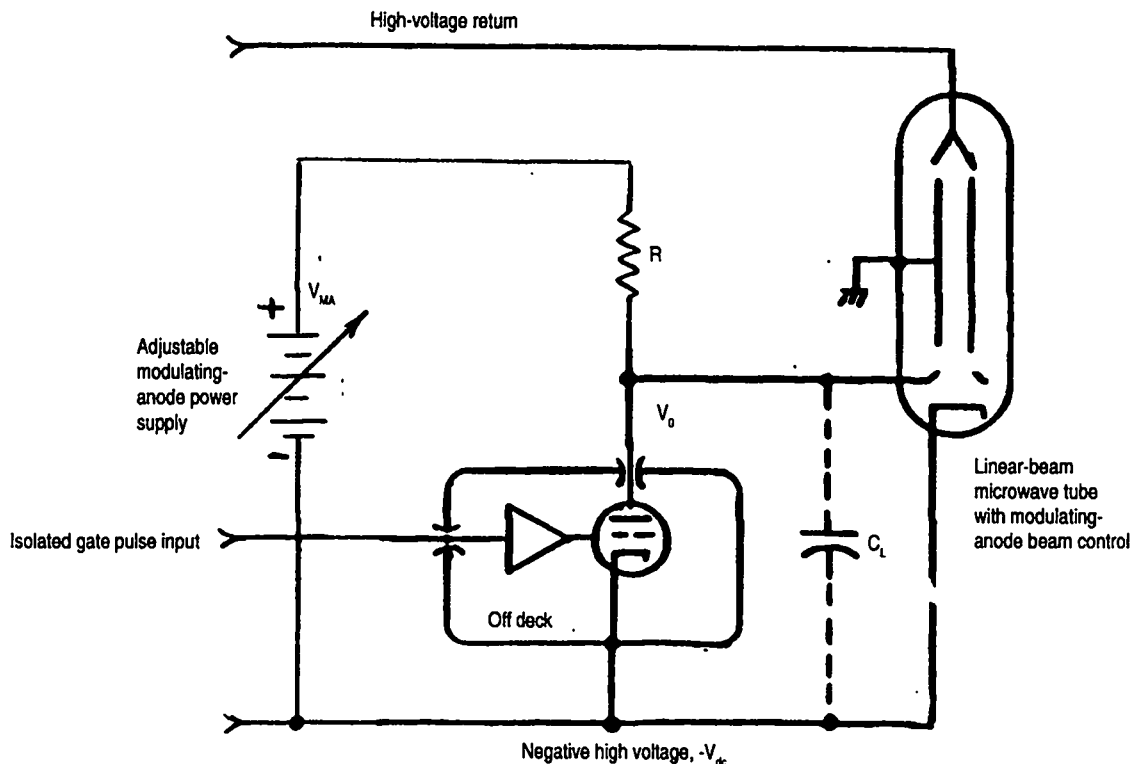


Figure 11-1. Modulating-anode pulser with passive pull-up and active pull-down.

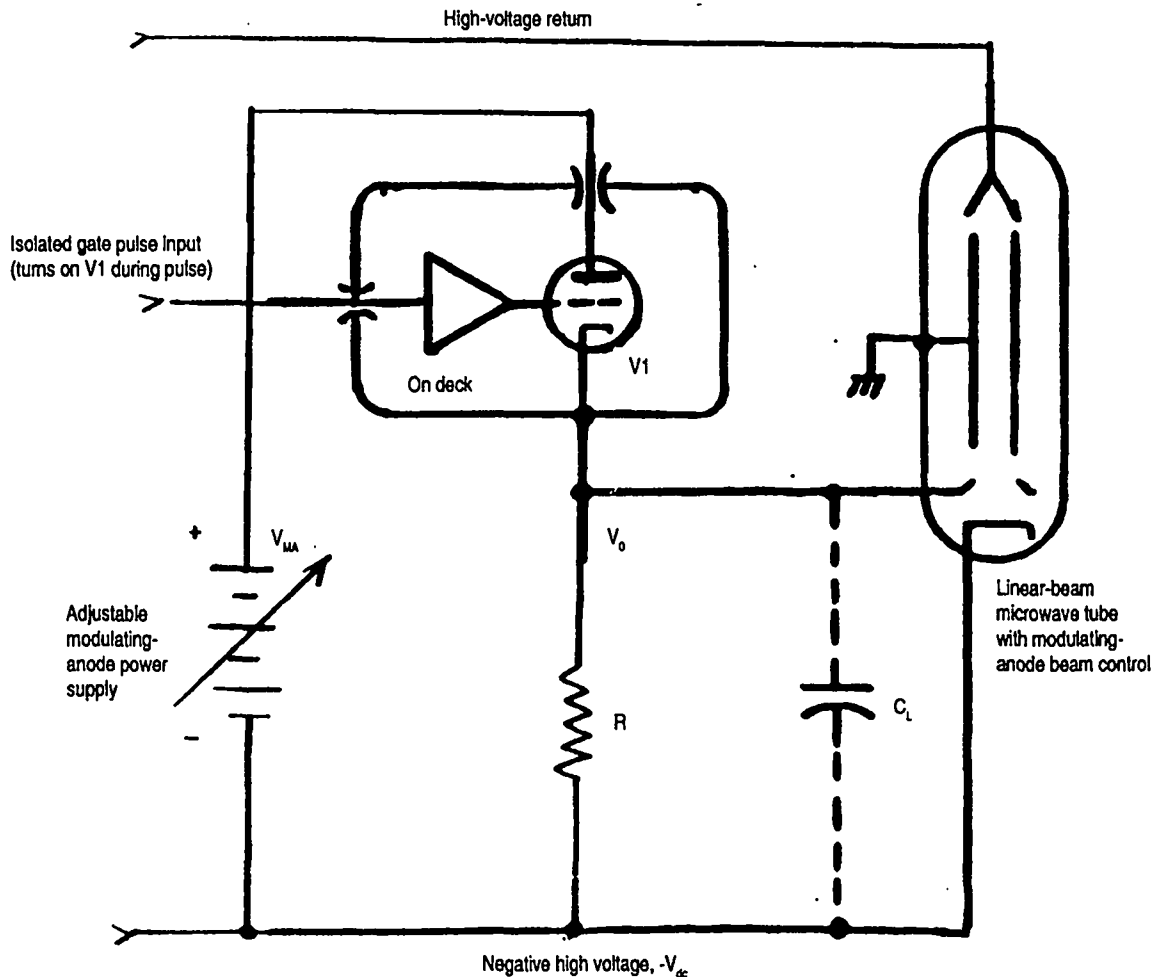


Figure 11-2. Modulating-anode pulser with active pull-up and passive pull-down.

(hence the term "floating-deck" modulator). The high-voltage pulse output is taken from this deck. The low-level circuits, therefore, are pulled up by their bootstraps, so to speak.

The pull-down resistor  $R$  now determines the pulse fall time. Its peak current may still be relatively high, as in the previous example, but the average current and dissipation will be proportional to the duty factor, which is seldom greater than 10% and is often less than 1%. However, for the same time-constant given in the previous example,  $R$  will have to be smaller. This is due to the fact that, all other things being equal, the load capacitance will be greater because it now includes the capacitance of the pulse deck, its power isolation transformer, and whatever capacitance is associated with isolating the low-level drive signal, which now has a common-mode voltage equal to the pulse-output voltage. The common-mode voltage must be rejected.

There are two components of power dissipation in both the switch tube and the pull-down resistor. One is proportional only to the duty factor and the other only to repetition rate. The dissipation in the resistor during the pulse is the most obvious. It is  $V_0^2/R$ , where  $V_0$  is the output-pulse amplitude. The average dissipation component is this peak power multiplied by the duty factor. The

corresponding component of switch-tube dissipation is the anode-cathode voltage drop—which is required to sustain the intrapulse resistor current—multiplied by the current. The average is this peak anode dissipation multiplied by the duty factor. At the beginning of each pulse the load capacitance  $C_L$  must be charged to a voltage  $V_0$ , giving it an energy change of  $1/2 C_L V_0^2$ . An equal amount of energy is dissipated in the switch tube each pulse to accomplish it. The average-power dissipation component is the per-pulse energy multiplied by the pulse repetition rate. At the end of each pulse, the same amount of capacitor energy is dissipated in the resistor (regardless of its value) in the act of discharging it to its pre-pulse voltage level. The average-power component is the per-pulse capacitor energy multiplied by the repetition rate. We can see that both duty factor and PRF are independently stressful operating characteristics. Neither can be ignored.

The average current that flows through the modulator circuit, either from the main high-voltage power supply, or from the adjustable amplitude-control supply, is the sum of the duty-factor-proportional component,  $V_0/R \times DF$ , and the repetition-rate-proportional component,  $V_0 \times C_L \times PRF$ . Where fast rise-and-fall times, high-duty factor, and high PRF are required, the average current and dissipation can become prohibitively high, leading us to the next modulator topology.

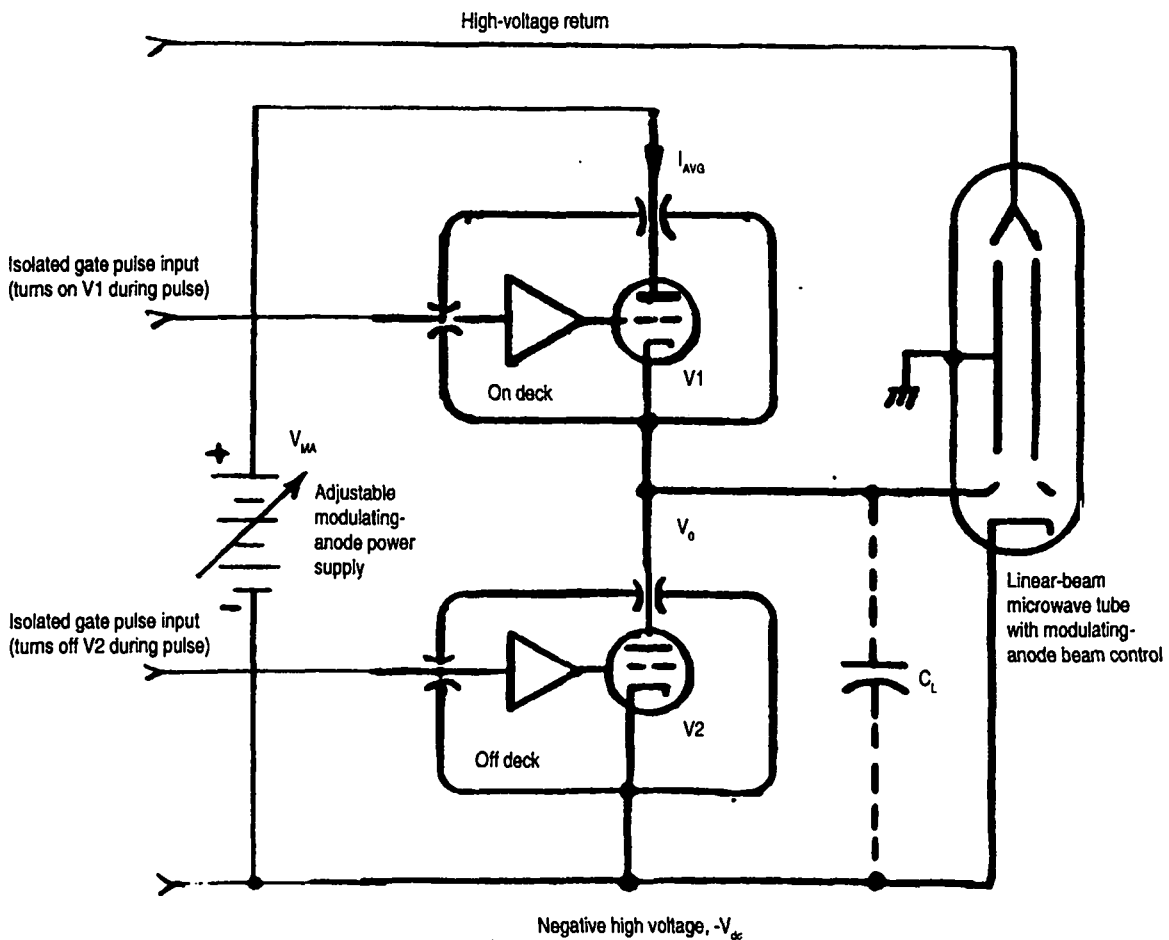


Figure 11-3. Modulating-anode pulser with active pull-up and active pull-down.

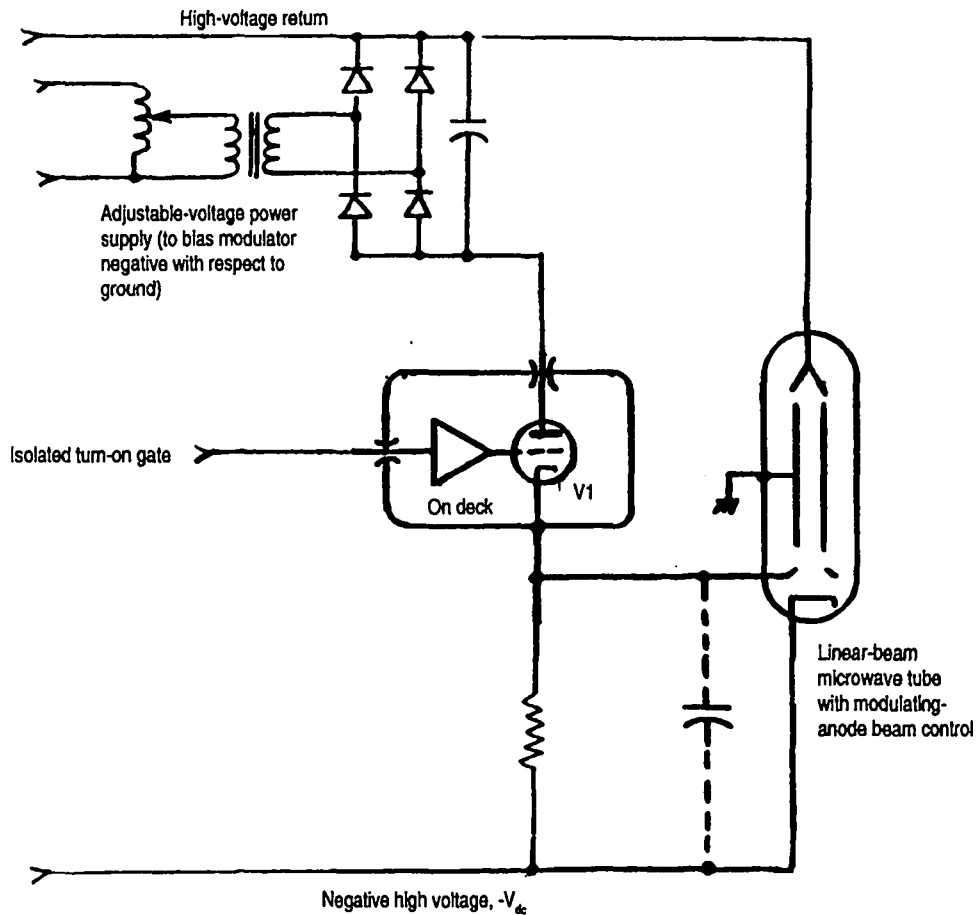


Figure 11-4. Alternative modulator amplitude control (why is this not likely to be a good idea?)

### 11.1.3 Active pull-up and pull-down

The topology of Fig. 11-3 has both active pull-up and pull-down, and the low-level gating strategy is such that the tubes never conduct simultaneously. This obviates a "shoot-through." If there is no resistive component to the load, such as modulating-anode interception current, there are no average current or dissipation components that are proportional to duty factor. All that is left are the PRF-proportional stresses. Both switch tubes experience average dissipation of  $1/2 C_L V_0^2 \times PRF$ , and the average modulator current is  $V_0 C_L \times PRF$ . The pulse rise-and-fall times depend entirely on the peak current available from the switch tubes, which, especially if they are tetrodes, will be nearly constant throughout most of the transition intervals until the diode-line voltages of the tubes are reached. After these voltages are reached, the current will fall off dramatically, and the time required for the last few percentages of voltage will be quite protracted. The initial rates of voltage rise-and-fall will be  $I/C_L$ , where  $I$  is the initial peak-anode current. Versatile, high-performance modulating-anode pulsers are almost always of this basic type.

However, if the type of power supply shown is used and variable amplitude control is desired (especially for high-ratio output, where pulse voltage is a large percentage of the load cathode voltage), then this topology can result in a discon-

certingly large amount of equipment, particularly if the modulator must operate at high PRF into large load capacitance. This situation raises the temptation to develop another circuit connection.

#### 11.1.4 An attempt at simplified amplitude control

In the circuit of Fig. 11-4, the variable-amplitude power supply is now referenced to the positive return rather than the negative high voltage. If the modulator output is a large percentage of the beam voltage, the potential saving is obvious. Many modulators incorporating this strategy have actually been built. The problem is they often don't work, and the reason is obvious enough. The modulator current must pass through the amplitude-control power supply in the wrong direction and is, therefore, blocked by the rectifier diodes. In most such cases, however, the power supply has a bleeder resistor across it that modulator current will go through. If the resistor value is low enough so that the voltage produced across it by the average modulator current is not greater than the adjustable-power-supply output voltage, the circuit will work. When the pulse/voltage ratio is higher than 50%, it makes more sense to "buck," using a power supply referenced to the ground side, rather than "boost," using a power supply referenced to the negative high voltage, which is what the next circuit facilitates.

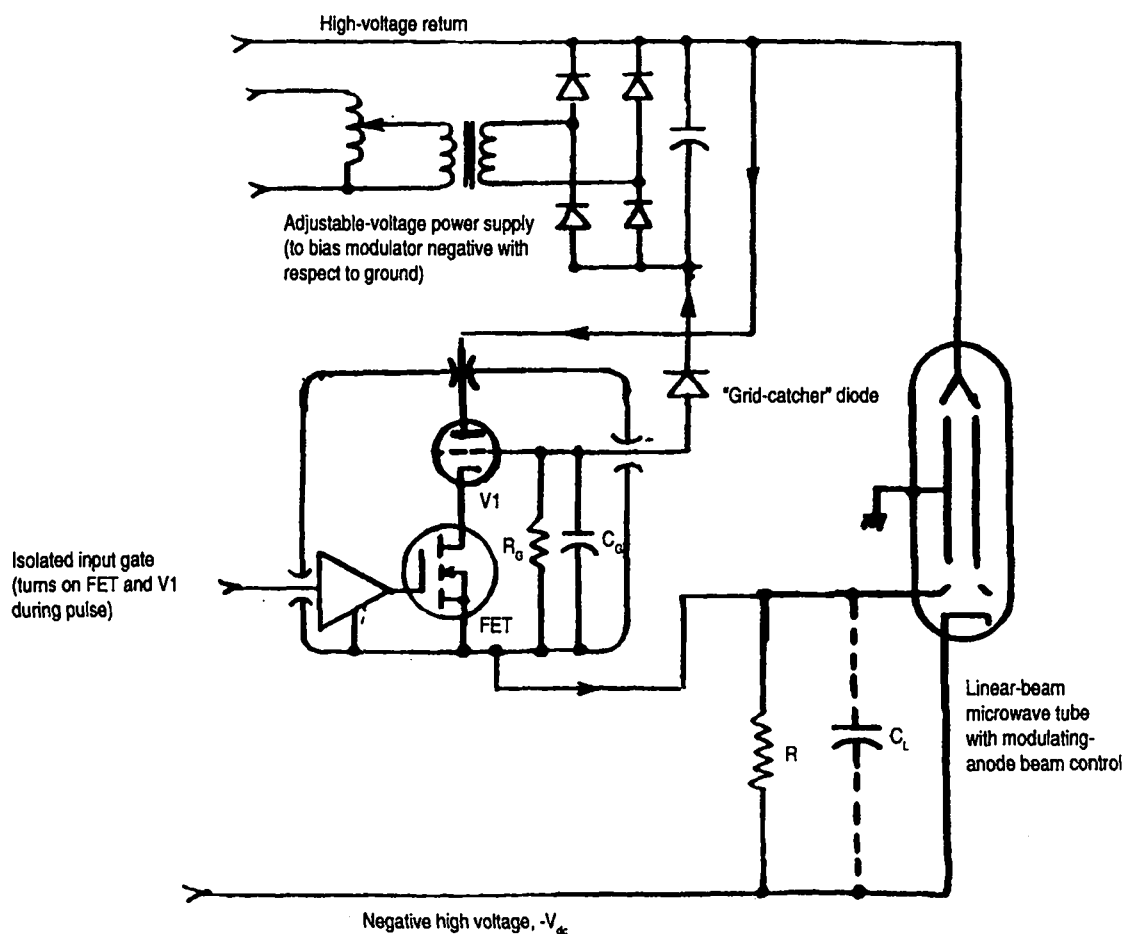


Figure 11-5. Another method of achieving modulator-amplitude control: the on-deck "grid-catcher" circuit.

### 11.1.5. The grid-catcher type of amplitude control

In Fig. 11-5 we see another active pull-up connection. Pull-down can be either active or passive, it doesn't matter. The "on" switch tube,  $V1$ , is cathode-driven by means of an FET in its cathode (as described earlier). The FET frees the grid of the tube for other purposes. In this case, grid voltage is returned to the deck potential through resistor  $R_G$ , which is shunted by capacitor  $C_G$ . The grid is also connected via a "grid-catcher" diode to the negative terminal of an adjustable dc power supply, whose positive terminal is connected to the positive return of the high-voltage power supply. During the interpulse interval, the FET is turned off, and the voltage at its drain rises so that the positive voltage at the cathode of  $V1$  is sufficient to cut it off. At the beginning of a pulse, the FET is driven into conduction, which pulls the cathode of  $V1$  near deck potential, which is also grid potential. The switch tube will conduct zero-bias anode current, charging up the load capacitance  $C_L$  at an initial rate of  $I/C_L$ , where  $I$  is the initial zero-bias anode current. When the output voltage attempts to become more positive than the voltage at the negative terminal of the amplitude-control power supply, the grid-catcher diode becomes forward-biased and begins to conduct, providing an alternative path for  $V1$  output current. To pass through the diode, however, the current must also pass through  $R_G$  and  $C_G$ , charging up  $C_G$  in the direction that makes the grid of  $V1$  negative with respect to its cathode, shutting it off again. (Note that this current is also in the proper direction through the amplitude-control power supply.) The output-pulse flat top will stop at a voltage with respect to ground that is more positive than the amplitude-control voltage by the amount of negative grid bias required to cut off  $V1$  anode current. For instance, if the amplitude-control power-supply voltage was set at -10 kV and it takes a negative bias of 500 V to cut off  $V1$ , the modulating-anode pulse voltage will have a flat-top that is 9.5 kV negative with respect to ground.

During the flat-top portion of the output pulse,  $V1$  functions as a cathode follower. Up to its limit, it will conduct whatever intrapulse current is required by the modulating anode or anodes. The only change in output voltage is the change in  $V1$  grid-cathode voltage required for the current change. (The larger the  $V1$  transconductance, the smaller the voltage change.)

If the grid-catcher diode were a perfect component with no shunt capacitance, there would be no need for the shunt capacitor  $C_G$  in the grid circuit of  $V1$ . Because there is capacitance across the diode, there will also be convection current through it during the rise-and-fall intervals of the pulse. This current would also flow through  $R_G$ , producing voltage across it that would tend to reduce the amount of anode current from  $V1$ . The negative voltage across  $R_G$  would be

$$\frac{dV_o}{dt} \times C_D \times R_G,$$

where  $C_D$  is the shunt-diode capacitance. Therefore, the value of  $R_G$  would, in effect, determine the rate-of-rise of the output pulse because it is  $I/C_L$ , where  $I$  is the  $V1$  anode current.

The capacitor  $C_G$  integrates the  $dv/dt$  current, making it a smaller replica of the output-pulse rise-time wave shape. With a  $C_G$  large enough, the voltage

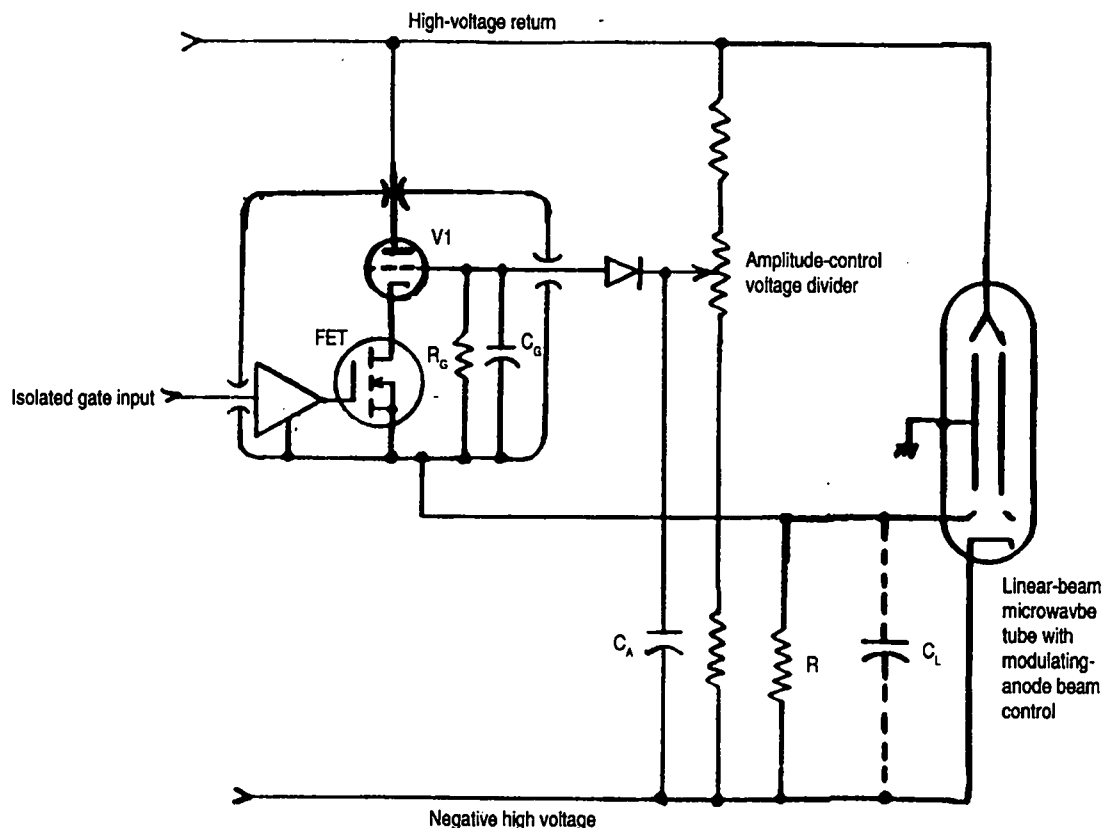


Figure 11-6. "Grid-catcher" type of modulator-amplitude control with passive voltage-divider adjustment.

across it can be made to have negligible effect on the  $V1$  available current. The optimum value is usually experimentally determined, starting with one based on a reasonable estimate of diode capacitance—say, 5 pF—and reduced from that value successively until an effect on rise time can be discerned. If the switch tube is a triode, as shown, then note that its anode-grid capacitance will have the same effect as the diode capacitance and will have to be included with it. Both are magnified, in effect, by the "Miller" effect. The magnitude of  $C_G$  determines the value of  $R_G$ , which must be small enough so that  $3 R_G C_G$  is less than the shortest interpulse interval. The value of these two components determines the average current that the amplitude-control power supply must handle. Once again, there are duty-factor and PRF-dependent components of the average current of the control power supply. The peak current through  $R_G$  is  $V_G/R_G$ , where  $V_G$  is the negative voltage required to cut off  $V1$  anode current. The average-current component is this peak current multiplied by the duty factor. An amount of charge,  $C_G V_G$ , must be passed through  $C_G$  as each pulse top is established. The average-current component from this is  $C_G V_G \times PRF$ . The total control-power-supply average current is the sum of the two components.

#### 11.1.6 The grid-catcher circuit with potentiometer-type control

Figure 11-6 shows an alternative to the amplitude-control power supply: an amplitude-control voltage divider. The potentiometer is obviously not just a simple, commercially available variable resistor. It is custom made. At least one

motor-driven version has been built using a multitude of small individual resistors in series with tap points between them. A screwlike mechanism driven by the motor moves the output lead from one tap point to the next in make-before-break fashion. The resistance of the voltage divider must be small enough so that the average diode current does not substantially alter the voltage at the tap point as duty-factor or PRF vary, as discussed above. The bypass capacitor  $C_A$  is made large enough so that the intrapulse value of diode current does not seriously alter the voltage across it. Note that this capacitor is referenced to the microwave-tube cathode voltage, which is subject to intrapulse droop as its beam current is removed from the main capacitor bank. This droop component is coupled by means of  $C_A$  to the amplitude-control tap point of the voltage divider. The modulating-anode pulse voltage, therefore, will track the negative high voltage, keeping the intrapulse beam current of the microwave-tube load essentially constant. (In fact, if  $C_A$  is not large enough, it will be charged up by the intrapulse diode current, and the modulating-anode pulse will actually rise with respect to the negative high voltage.)

#### 11.1.7 *The gate-catcher type of amplitude control*

The circuits shown in Figs. 11-5 and 11-6 do not permit  $V1$  to be operated with positive grid voltage. Often  $V1$  is a tetrode, in which case adequate anode current is usually obtained with zero or slightly negative grid bias. But this is seldom the case with a power triode. Figure 11-7 shows how, with the addition of an additional FET stage in the  $V1$  cathode circuit, any amount of effective positive grid drive can be introduced, as long as it is consistent with the drain voltage hold-off of the two FET switches. Even though the two FET switches are in series, they do not share the interpulse hold-off voltage at the cathode of  $V1$  because they turn on and off at different times.

In the circuit illustrated,  $Q3$  is the timing switch. Its gate drive responds to the optically coupled low-level turn-on gate at the input to fiber-optic-receiver,  $U1$ . The gate of  $Q3$  is driven from an active pull-up/pull-down transistor pair,  $Q1$  and  $Q2$ , that provides active source and sink for the  $dv/dt$  currents between the drain and gate of  $Q3$ . (These currents are akin to the "Miller" capacitance effect in a triode vacuum tube.) The  $Q3$  circuit is a true bootstrap circuit, having its own isolated 15-Vdc power source, which is a high-isolation, low-input/output-capacitance dc-dc converter.

The other FET cathode switch,  $Q4$ , is already biased into conduction before a pulse begins. This is accomplished by the current flowing through  $R1$  and  $R3$  from a 24-Vdc source, which is also a high-isolation dc-dc converter. Zener diode  $CR5$  clamps the  $Q4$  gate voltage at +15 V. Even though  $Q4$  is in the conducting state prior to the low-level input gate pulse,  $Q3$  is still cut off, which keeps  $V1$  cut off as well. The grid of  $V1$  is "grounded" in that it is connected to the floating deck, from which the high-level pulse output is obtained. The cathode of  $V1$  is not directly connected to the drain of  $Q3$ . (Because  $V1$  in this case has a directly heated cathode, the cathode connection is made at the secondary center-tap of the filament transformer,  $T1$ , which is the electrical mid-point of the ac filament circuit.) Between the cathode and the  $Q3$  drain is a dc power source comprising a bridge rectifier,  $CR1-4$ , and filter capacitor,  $C1$ . The ac input is

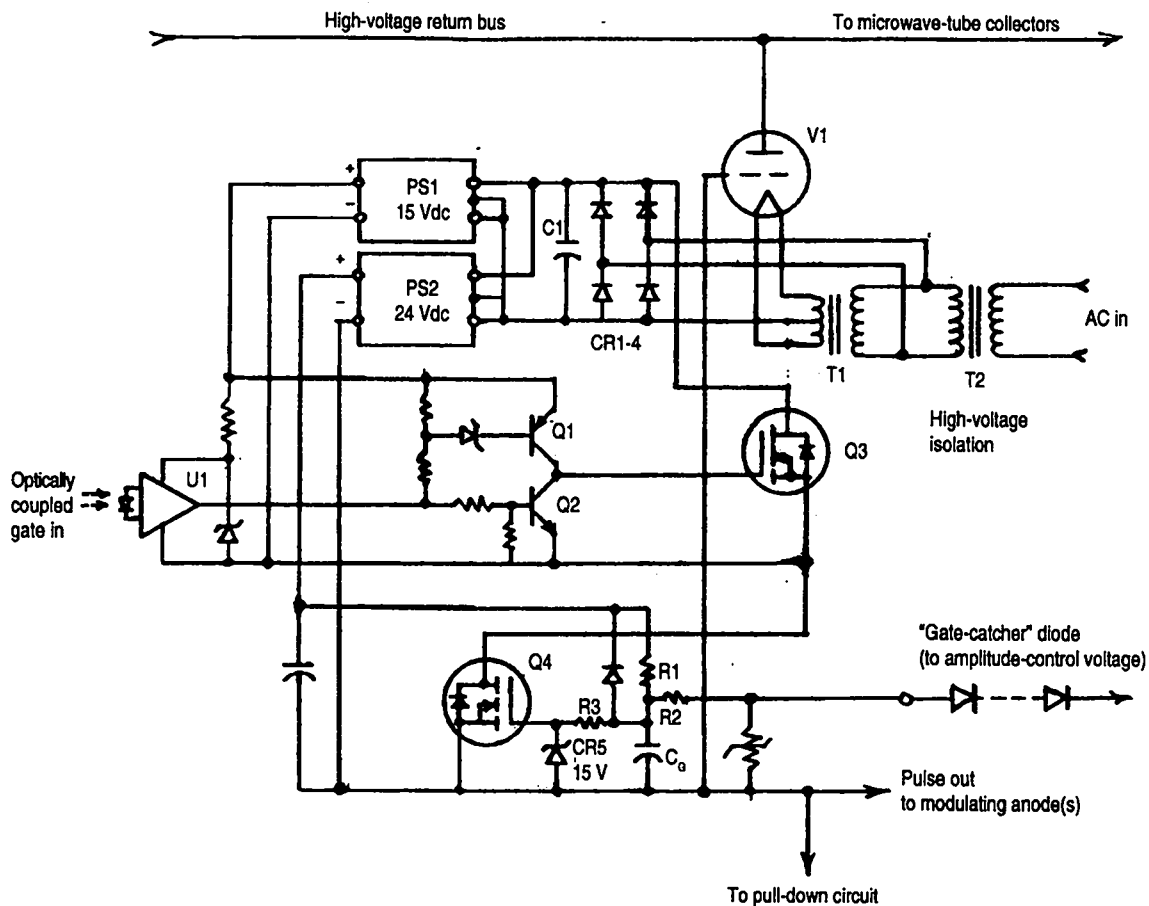


Figure 11-7. "Gate-catcher" circuit permitting switch-tube positive-grid control.

provided by the secondary winding of T2, the high-voltage isolation transformer. By coordinating with the primary voltage required of T1, the secondary voltage of T2 can be whatever is needed for the dc across C1 to be the desired amount of positive grid bias for V1. It is not applied to the grid, however. This voltage is applied to the cathode of V1 as negative voltage when Q3 is pulsed into conduction in response to the input timing gate. The entire cathode current of V1 must pass through this power supply, not just the grid current. During the interpulse interval, Q3 must hold off whatever cathode voltage is required to keep V1 cut off in addition to the bias voltage across C1.

Once Q3 is turned on at the beginning of an output pulse, conduction commences through V1, Q3, and Q4 (which was already on) to charge up the external load capacitance. When the output pulse, which increases from an interpulse value at or near the negative high voltage toward ground potential, reaches whatever voltage the anode of the "gate-catcher" diode string is connected to, an alternative current path through C<sub>G</sub> and R2 becomes available. When this path is utilized, C<sub>G</sub> rapidly discharges, shutting off Q4 and stopping the flow of load current, even though Q3 is still biased into its conducting state. The gate of Q4 now plays the same role in controlling output-pulse amplitude that the grid of V1 used to play.

Between pulses, C<sub>G</sub> is recharged through R1, which is considerably smaller in

value than  $R3$ , to nearly 24 V, but the gate of  $Q4$  is clamped to 15 V. Therefore, during the pulse rise time, the  $dV/dt$  current, which will flow in the stray capacitance shunting the control diode string, can discharge  $C_G$  by 9 V before any effect is noted in the state of conduction of  $Q4$ , thus permitting  $C_G$  to be made a smaller value than if it were directly connected to the  $Q4$  gate.

### 11.1.8 The "quasi-resonant" modulating-anode pulser

So far, we have discussed circuit refinements that have reduced the operating stress levels to those proportional to load capacitance, pulse-repetition frequency, and the square of the output voltage. The product of these values will determine both the average-power dissipation in the modulator switches and the external average power required for the modulator to operate.

It is possible to contemplate a combination of parameters that results in power consumption and dissipation so high that the overall design becomes impractical, if not ridiculous. The topology shown in Fig. 11-8 may then become practical. Its obvious drawback is its complexity. It uses four electronic switches instead of two in the designs previously discussed. Its single, but perhaps crucial, advantage is that it provides true switch-mode application of the electronic switches. The load-capacitance charging- and discharging-current amplitudes are limited not by resistance, either internal or external to the switch tubes, but by reactance. This means that switching can be accomplished without power dissipation. During the leading edge of each pulse, both charge and energy are removed from capacitor  $C2$ , which is maintained at a voltage (with respect to the negative high voltage) that is one-half of the desired output-pulse amplitude.

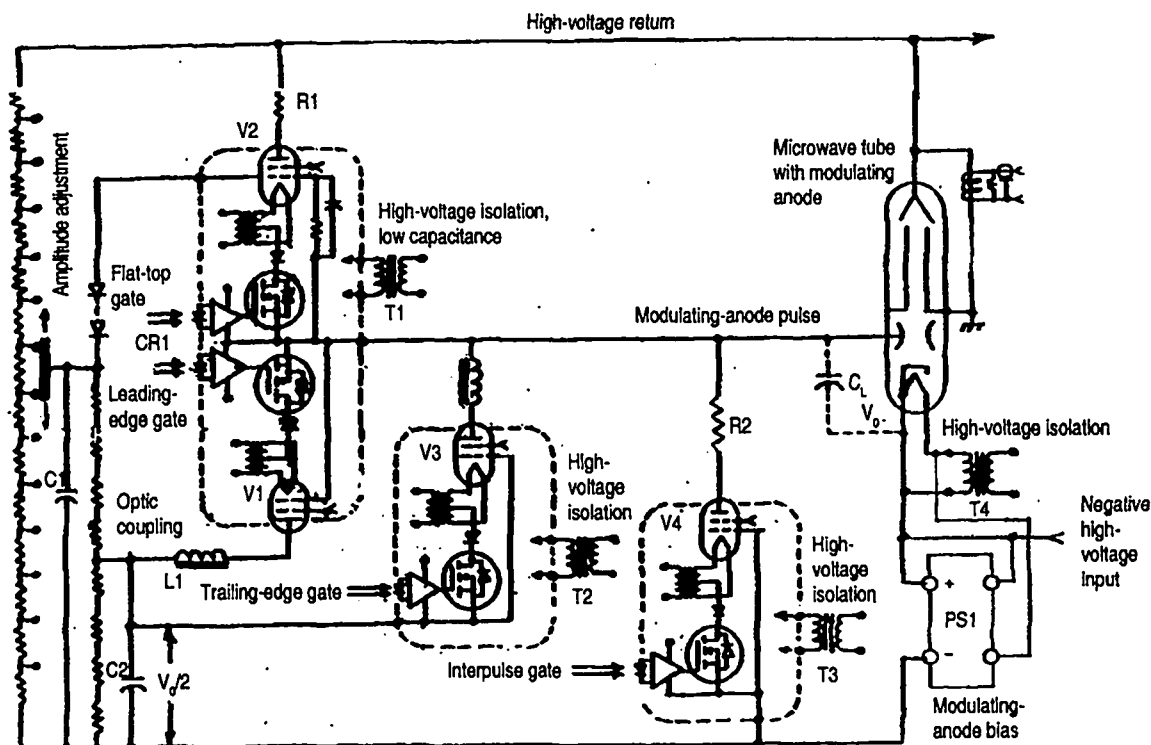


Figure 11-8. "Quasi-resonant" charge-and-discharge modulating-anode pulser.

The energy and charge are transferred to the load capacitance  $C_L$  through  $L1$  and  $V1$ . Switch tube  $V1$  is driven into a state of conduction such that its anode-voltage drop at the peak charging current is small with respect to the pulse output voltage. The smaller the switch-tube voltage drop, the less energy it will dissipate each pulse. Also the closer the charging-circuit impedance will approach

$$\sqrt{\frac{L1}{C_L}},$$

and the closer the peak current will approach

$$\frac{V_0}{2} \sqrt{\frac{L1}{C_L}}.$$

The output across  $C_L$  will be in the form of an inverted cosine wave for half a cycle, as shown earlier in Fig. 9-11. This wave described the dc-resonant charging of the capacitance of a pulse-forming network. The rise time, from zero to 100% of  $V_0$  (which approaches 200% of the voltage across  $C2$ ), is

$$\pi\sqrt{L1 \times C_L}.$$

The smaller the inductance of  $L1$  can be made, the greater the peak current becomes—but the shorter will be the rise time. The current in the circuit is in the form of a half-sine wave. For this reason, even though  $V1$  is shown in the form of a full-control electronic switch, it need not be. A half-control switch will be automatically commutated to the off state when the output voltage reaches 100% and the charging current attempts to reverse polarity. The switch (or a diode in series with it) must be capable of blocking a reverse voltage of  $1/2 V_0$  as soon as the rise time is completed and the voltage across  $L1$  collapses.

If we ignore for a moment the conditions during the flat-top portion of the output pulse, we can proceed directly to the trailing edge of the pulse, which is initiated by driving the discharge switch tube  $V3$  into conduction in response to the optically coupled trailing-edge gate. The discharge path includes  $C_L$ ,  $V3$  (and its cathode-drive FET), and  $L2$ , whose rise-and-fall time performance is identical with  $L1$ . Current in this path restores to the source-energy store  $C2$  the charge and energy that were removed from it during the rise time of the pulse. In fact, if the flat-top portion of the pulse were of zero length, the current through  $C2$  and  $C_L$  would be a complete cycle of a sine wave, with the positive-going half flowing through  $L1$  and  $V1$  and the negative-going half flowing through  $L2$  and  $V3$ . The output voltage  $V_0$  across  $C_L$  would be in the form of a complete cycle of an inverted cosine wave, having a peak value of  $V_0/2$ , and, of course, a peak-to-peak value of  $V_0$ , which is the output voltage we want.

Because we have produced sinusoidal waveforms by using two unidirectional switches conducting in time sequence, now we can delay the two half-cycles by

as much time as we choose (*sinusoidalus interruptus*), providing that we don't lose too much charge from  $C_L$  during the flat-topped portion of the pulse. This is the function of  $V_2$ , which comes into conduction only when  $C_L$  has been fully charged. It acts as a trickle charger to provide whatever intrapulse leakage currents there might be, including actual beam-current interception by the microwave-tube modulating anode. (Even as little as 0.1% of a lot can be something.) Note that a grid-catcher diode,  $CR1$ , is used to coordinate the output voltage of the  $V_2$  circuit with the "ring-up" voltage on  $C_L$  produced by the  $V_1$  circuit. Capacitor  $C1$  acts as the energy store for the grid-clamp diode current. Switch tube  $V_2$  is the only one that must hold off the entire beam voltage of the microwave tube. The current it must handle, however, is a small fraction of what  $V_1$  and  $V_3$  must handle. For this reason, external resistance can be included in the anode circuit of  $V_2$  that can be made high enough in value so that arc-through current can be made almost negligibly small.

The final switch tube,  $V_4$ , conducts throughout the interval between the end of the discharge portion of one pulse and the beginning of the charge-up portion of the next. It provides a sink for whatever leakage currents there might be, including leakage across the ceramic insulator between modulating anode and body of the microwave tube. The leakage would otherwise tend to pull the modulating anode positive with respect to the cathode. (Note that a small positive interpulse modulating-anode voltage can be particularly devastating to a microwave tube because it gives rise to a minuscule amount of cathode current that is super-focused as it transits the length of the microwave tube. It then bores a very small hole right through the beam collector.) For this reason it is customary to provide a modest amount of modulating-anode bias voltage (1 kV to 2 kV) in order to assure that the modulating anode is negative with respect to the microwave-tube cathode throughout the entire interpulse interval. (This is the function of  $PS1$ .) The ac input to such a supply is often derived from the filament voltage of the microwave tube, as shown. Switch tube  $V_4$  must be capable of holding off the full pulse voltage,  $V_0$ , which is usually less than the full microwave-tube beam voltage. The current that it must handle is typically less than that of  $V_2$ , so resistance  $R2$  can be added to its anode circuit, serving the same purpose as  $R1$ .

It would be possible to configure the circuit so that a single inductor would suffice. It takes two inductors, however, to insure that all capacitive charging currents, including that of the floating-deck that is common to  $V_1$  and  $V_2$ , are limited by series-resonant impedance rather than by switch-tube internal resistance. Part of the total load capacitance that must be charged and discharged is the primary-to-secondary capacitance of the high-voltage power isolation transformer,  $T1$ . So it is important that this transformer be of low-capacitance design. The two other decks and the microwave-tube filament also require high-voltage isolation of the ac input power provided by  $T2$ ,  $T3$ , and  $T4$ , but interwinding capacitance is of no particular importance, because the decks are referenced to nominally fixed voltages.

The modulator of Fig. 11-8, therefore, can actually be seen as a hybrid of two separate modulators. The first, using switch tubes  $V_2$  and  $V_4$ , can be seen to be a conventional active-pull-up, active-pull-down floating-deck pulser. Its role has

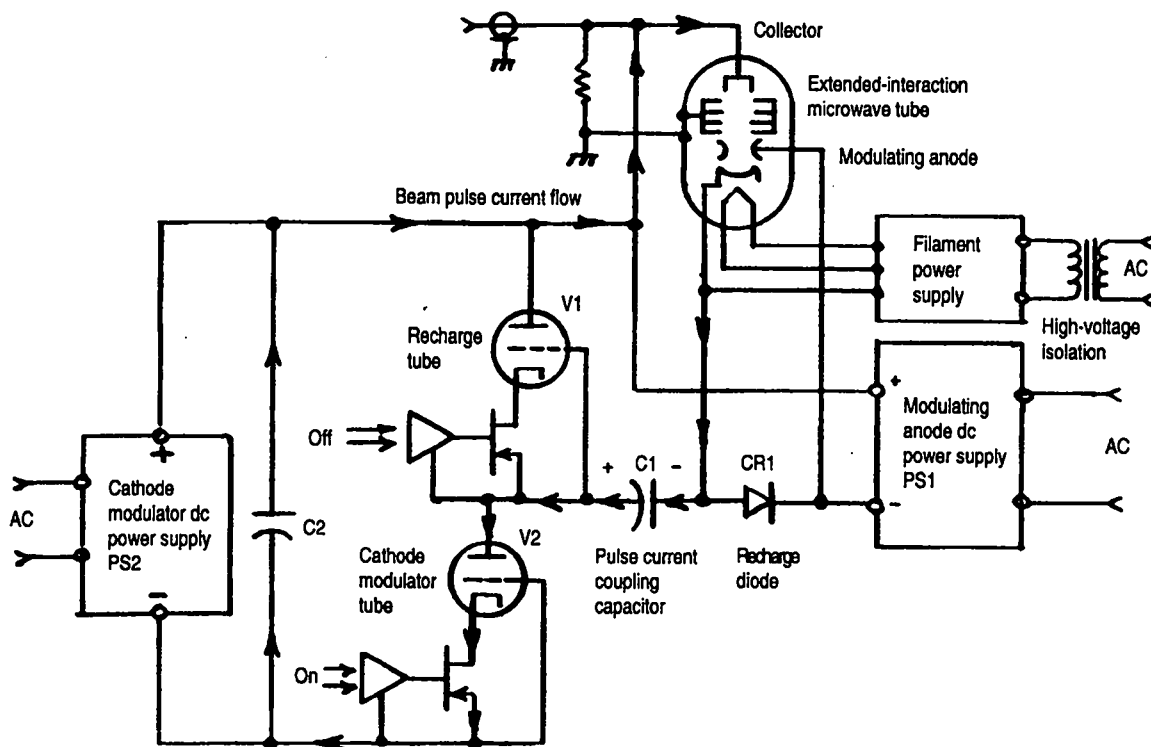


Figure 11-9. Hybrid modulating-anode pulser for velocity-jump guns (conditions during pulse).

been relegated to holding the flat-top of the output pulse up (V2) and the flat bottom of the interpulse interval down (V4). The other modulator is a quasi-resonant, or interrupted-resonance, capacitor-charging and -discharging circuit that comprises switch tubes V1 and V3 and resonating inductors L1 and L2, which operate from a secondary energy and charge store maintained at a voltage approximately 1/2 of the desired output pulse voltage. None of the switch tubes conduct simultaneously, so four separate, low-level timing signals are required, as shown. This is certainly not a simple modulator configuration, but it is able to satisfy otherwise unattainable performance requirements.

#### 11.1.9 The modulating-anode power supply/cathode-pulser hybrid

Also in the category of hybrid is the arrangement shown in Fig. 11-9. It is best suited for microwave tubes that have "velocity-jump" electron guns and are characterized by a modulating-anode pulse voltage that is around half the cathode voltage. Extended-interaction oscillators and amplifiers that operate at moderate power levels are usually in this category.

In this case, there is no modulating-anode pulser as such. The microwave-tube modulating anode is connected to the negative terminal of a dc power supply, PS1, the positive terminal of which is connected to the collector (virtually at ground). During a pulse, the supply-output voltage continuously biases the modulating anode to the level that a conventional pulser would, except that its reference point is ground instead of cathode voltage. (This is really no different than the circuit of Fig. 11-5, except that there is no switch tube and no grid-catcher diode.) There is no beam current in the tube yet, because switch tube V2

and its cathode-drive FET block its path. The anode of the switch tube is connected to the cathode of the microwave tube through a coupling capacitor,  $C1$ . During the interpulse interval, the anode of  $V2$  is maintained at a voltage close to ground by conduction through the "recharge" tube,  $V1$ , which can be replaced by a resistor if the operating duty factor is low enough. Diode  $CR1$  keeps the cathode of the microwave tube positive by the amount of the diode drop (with respect to its modulating anode), which means that the average value of voltage across  $C1$  is equal to the modulating-anode voltage as well.

To initiate a beam-current pulse, switch-tube  $V2$  is driven into conduction in response to the optically coupled "on" gate, while  $V1$  is driven from the conducting to the non-conducting state. The cathode-modulator dc power supply  $PS2$  has an output voltage slightly larger (by the amount of the conduction anode-voltage drop of  $V2$ ) than the voltage by which the cathode of the microwave tube must be pulled negative (with respect to its modulating anode) for the desired amount of beam current. For a 50%-modulating-anode tube, this means that  $PS1$  and  $PS2$  have very nearly the same voltage ratings, each one-half of the microwave-tube beam voltage. When  $V2$  conducts, it pulls the positive end of  $C1$  negative by an amount slightly less than the  $PS2$  voltage. Assuming that  $C1$  has a sufficiently large capacitance, the negative end follows the positive end, and the cathode of the microwave tube, which was already negative by an amount equal to the  $PS1$  voltage, is pulled even further negative so that the intrapulse value is very nearly  $PS1 + PS2$  (assuming zero conducting-anode drop for  $V2$ ).

The path of pulse current is shown by the arrows. It includes  $C2$ , the microwave-tube collector-cathode path,  $C1$ , and  $V2$ . Figure 11-10 shows what happens between pulses. During the pulse, charge is removed from both  $C1$  and  $C2$  that is equal to

$$\int I \cdot dt,$$

where  $I$  is the peak-beam current and  $dt$  is the pulse duration. Except in long-pulse, high-duty-factor situations, there is negligible contribution to pulse current directly from the dc power supplies. Current from them restores the lost capacitor charge during the interpulse interval. There are two separate current components:  $I_1$  is current from  $PS2$  restoring the lost charge to  $C2$ ;  $I_2$  flows out of  $PS1$  through the recharge tube  $V1$ , which conducts during the interpulse interval, and through  $C1$  and  $CR1$ , restoring the lost charge to  $C1$ . The average values of the two currents are the same and equal to the time-averaged value of microwave-tube beam current. For some people, the only surprise of this arrangement is that the average current from a power supply connected to a modulating anode, which itself draws no current, is equal to the average beam current. In this case, the total power requirements of a 50%-modulating-anode-voltage tube are shared almost equally by the two dc power supplies, both in voltage and current. Regardless of the voltage split between modulating-anode voltage and cathode voltage (or the degree of "voltage jump"), the average currents from the two power supplies will be identical.

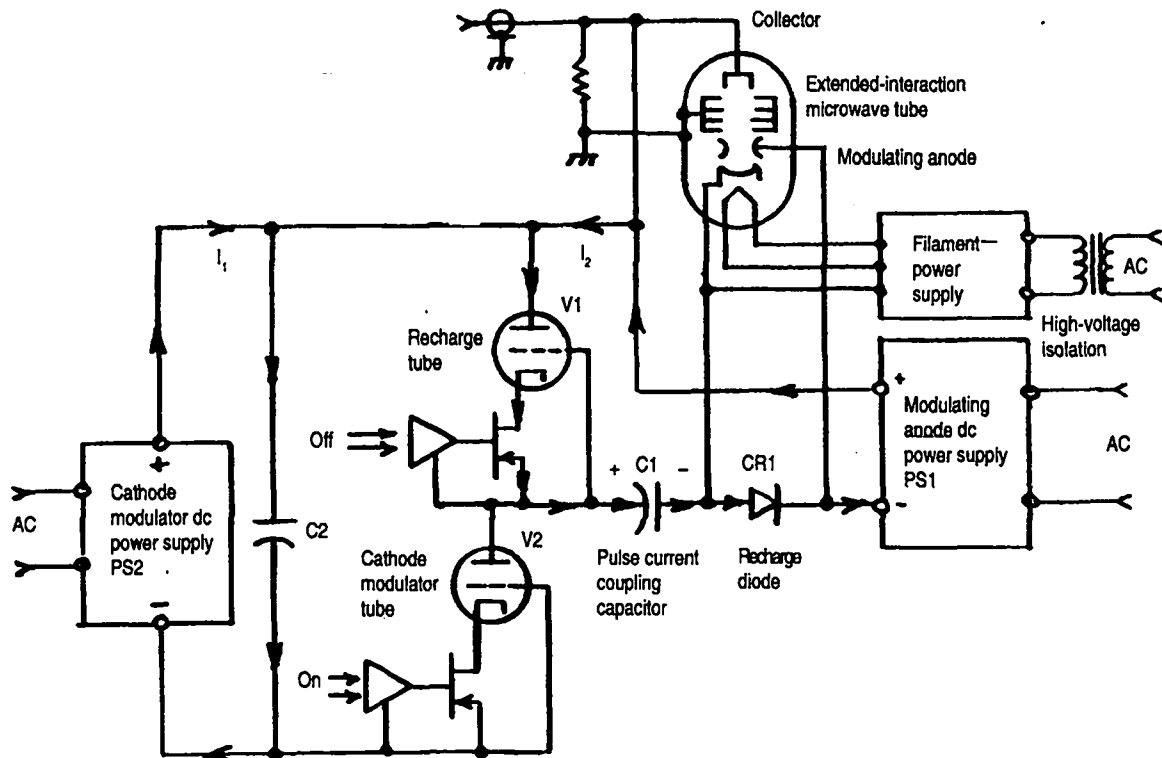


Figure 11-10. Hybrid modulating-anode pulser for velocity-jump guns (conditions between pulses).

## 11.2 The self-capacitance of modulator decks

If a significant portion of the load capacitance that a modulating-anode pulser must drive can be embodied in the electronic equipment deck associated with the pull-up vacuum tube, it stands to reason that a good design objective would be to minimize it. There is only one strategy that will do this: making the deck as physically small as possible and spacing it as far as possible from everything else, until the limiting case of corona-discharge threshold is reached. At this point, the deck will be a sphere of radius  $r$ . If  $V$  is the deck voltage,  $V/r$  must be less than the local-breakdown electric-field intensity for the medium in which it is immersed. (If, for instance, the medium is air, at standard temperature and pressure,  $V/r$  must be less than 30 kV/cm). However, practical considerations usually result in deck designs having dimensions that are considerably greater than the limiting case. (In these instances, the form factor looks more like a rectangular box with rounded corners than a sphere.)

Figure 11-11 is intended to provide an intuitive, as well as numerical, assessment of the difference in capacitance between a square-sided deck and the remotely located walls of a larger containment enclosure. The piece-wise approximation is based on the equivalent series capacitance of successive virtual-parallel-plate capacitors created by slicing up the space that extends outward from the deck surfaces, as shown by the dashed lines. Only one of the six contiguous volumes is shown. (Common surfaces are indicated by 45° angles.) If the length of each side is  $L$ , and we choose to slice up the space that progresses outward from each side into slabs of incremental thickness  $0.1L$ , then it can be seen that the dimensions of each successive slab are  $L(1 + 0.2n)$  on a side, where  $n$  is the

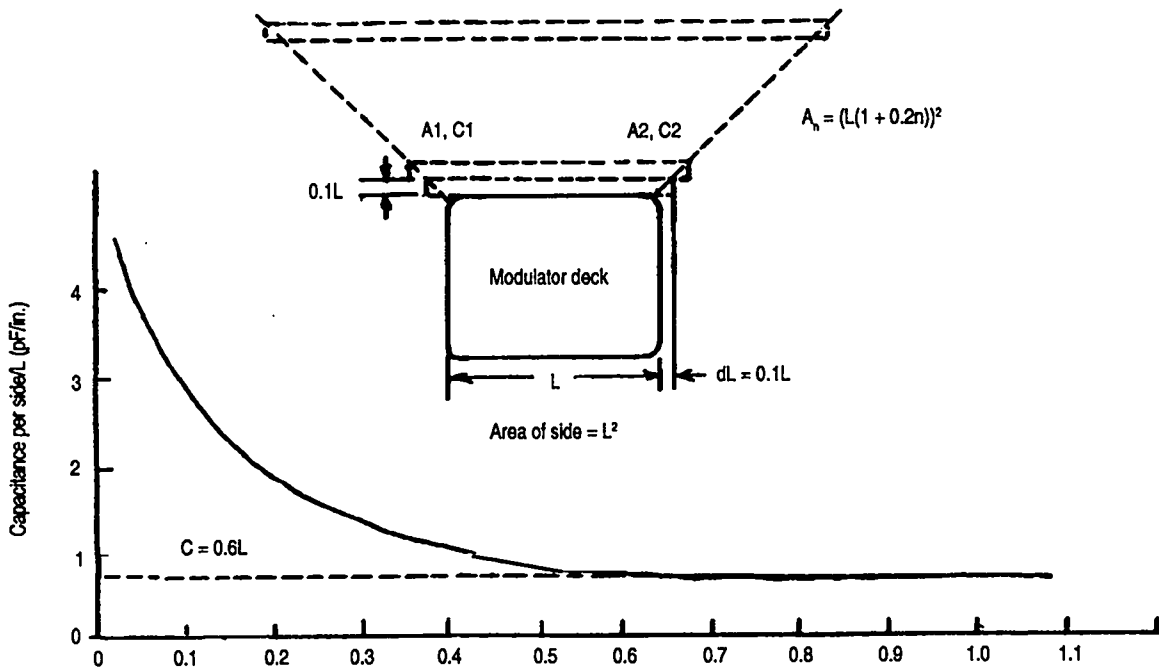


Figure 11-11. A method for determining modulator-deck self-capacitance.

number of the particular slab, with 1 being the closest one. Therefore, the area ( $A$ ) of each slab is  $L^2(1 + 0.2n)^2$ . Except for their ends, the dashed lines dividing up the slabs lie on electric-field equipotentials, so they could be replaced with conducting surfaces without altering the electric-field distribution. The parallel-plate capacitance between surfaces  $C_n$  is given as

$$\frac{0.225A_n \text{ pF/in.}}{0.1L}$$

normalized to the length of a side,  $L$ . The area, and therefore the parallel-plate capacitance, of each successive slab is greater than its immediate predecessor that is closer to the deck. The deck's total capacitance is the equivalent series capacitance of all of the incremental slabs, or

$$\text{Capacitance / side} = \frac{1}{\frac{1}{C_1} + \frac{1}{C_2} + \frac{1}{C_3} + \dots + \frac{1}{C_n}}$$

and

$$\text{Total capacitance} = 6(\text{capitance / side}).$$

Table 11-1 shows how the areas and capacitances of successive slabs increase,

n	Area/slice (in. <sup>2</sup> )	Capacitance/slice (pF)	Total Capacitance (pF)
1	1.41 L <sup>2</sup>	3.17 L	3.17 L
2	1.96 L <sup>2</sup>	4.41 L	1.84 L
3	2.56 L <sup>2</sup>	5.76 L	1.4 L
4	3.24 L <sup>2</sup>	7.29 L	1.17 L
5	4.0 L <sup>2</sup>	9.0 L	0.78 L
6	4.84 L <sup>2</sup>	10.9 L	0.73 L
7	5.76 L <sup>2</sup>	13 L	0.69 L
8	6.76 L <sup>2</sup>	15.2 L	0.66 L
9	7.84 L <sup>2</sup>	17.6 L	0.64 L
10	9.0 L <sup>2</sup>	20.3 L	0.62 L
11	10.2 L <sup>2</sup>	23 L	0.60 L
12	11.6 L <sup>2</sup>	26 L	0.59 L
13	13.0 L <sup>2</sup>	30 L	0.57 L

Table 11-1. How capacitance increases with slab area while series-equivalent total capacitance decreases with each additional slab.

and how the series-equivalent total capacitance decreases with each additional slab. But note that the total capacitance does not decrease very rapidly after about the eighth or ninth slab. This means if an outer wall is farther away than 0.8 or 0.9 times the deck length, it doesn't matter how far away it is—or what shape it is, either. The curve shows that capacitance per side is asymptotic to approximately  $0.6L$  pF. (This calculation assumes there is a relative dielectric constant of unity for the immersion medium, which certainly isn't true if the medium is dielectric oil.) An air-insulated deck, with dimensions of 6 in. on a side and with containment walls at least 5 in. away, can be expected to have a capacitance per side of approximately  $0.6 \times 6$  in., or 3.6 pF, and a total capacitance of approximately  $6 \times 3.6$  pF, or 22 pF. The same deck immersed in transformer oil that has a relative dielectric constant of 2 will have twice the self-capacitance. Increasing the size of the containment vessel will have virtually no effect on the deck self-capacitance, whereas changing the dimensions of the deck sides will have a direct effect on it.

Given that the deck will have to support at a minimum the modulator pull-up vacuum tube, the footprint of its tube socket will establish the minimum area for two of the deck sides. The largest single component that must be housed within the deck is usually the filament transformer for the switch tube. For this reason, the secondary voltage of the low-capacitance, high-voltage isolation transformer is sometimes made equal to the required filament voltage, thus eliminating the need for the filament transformer altogether. This, however, requires that other transformers within the deck be specially wound so that their primary voltages are also the same as the filament voltage. Transformer bulk can also be reduced by using higher-frequency primary power, such as the standard 400 Hz. Solid-state static inverters that operate at this frequency are readily available, as are many transformers of different designs. Even higher frequencies than 400 Hz are practical, but the advantages gained are seldom worth the high cost of the special-purpose components designed to exploit them.

### 11.3 Vacuum tubes appropriate for modulating-anode-pulsor service

The obvious performance criterion of a switch tube for modulating-anode-pulsor service is an adequate voltage hold-off capability. This, in turn, depends upon the circuit topology chosen (or invented) and the modulating-anode-voltage excursion required by the microwave tube, or family of such tubes involved. In reviewing the topologies previously discussed, we see that required voltage hold-off can range from one-half of the required voltage swing (the leading-edge and trailing-edge stages of a quasi-resonant modulator) to an amount equal to the full cathode voltage of the microwave tube (the pull-up tube of grid-catcher type connection).

The amount of peak-pulsed current required depends only upon the total load capacitance and the desired charge-and-discharge time intervals (rise time and fall time). The charge transport is the same for each pulse, so average current is determined by voltage swing, load capacitance, and pulse-repetition rate (unless the resistive pull-up or pull-down strategy is used). Average current, therefore, is independent of transmitter duty factor as such. Consequently, the switch-tube duty factor is usually a small fraction of transmitter duty factor. Tubes appropriate for this service, therefore, tend to be considerably smaller—electrically and physically—than those required for use as hard-tube modulators, such as beam-pulsors. Figure 11-12 shows the relative envelope sizes, compared with a 12-in. reference line, of some tube types that have been used in successful modulating-anode pulsors, even though they were not necessarily designed for such service specifically. (The tubes discussed are all members of families of similar tube types and are by no means the only ones worthy of consideration when contemplating a new application.)

#### 11.3.1 *The 4PR250C/8248 tetrode*

Labeled A in Fig. 11-12, this glass-envelope, radial-beam tetrode switch tube has seemingly been around forever and has graced the sockets of a multitude of air-insulated modulating-anode pulsors. Its anode-cathode voltage-hold-off capability is a very honest 50 kV, and although it is not rated for higher voltages, it has been known to tolerate more. Its long-life thoriated-tungsten filament will produce useful plate current greater than 4 A, and its radiation-cooled tantalum anode will dissipate 250 W. It is also relatively affordable, making it an excellent choice in pulsor designs operating up to 50 kV.

#### 11.3.2 *The 8960 tetrode*

The 8960 tetrode (B) is another glass-envelope, radial-beam tube with an honest 50-kV anode-voltage hold-off capability and a thoriated-tungsten, directly heated cathode. But it is physically and electrically larger than the 4PR250. It boasts 12-A peak-anode-current capability and 1200-W anode dissipation. It is often employed in air-insulated modulator designs up to 50 kV that are beyond the capability of the 4PR250.

#### 11.3.2 *The Y-847 triode*

A relatively modern tube, the Y-847 triode (C) has planar-electrode geometry and ceramic-metal construction that is especially designed for high-voltage service. Its construction makes it independent of orientation and tolerant of high

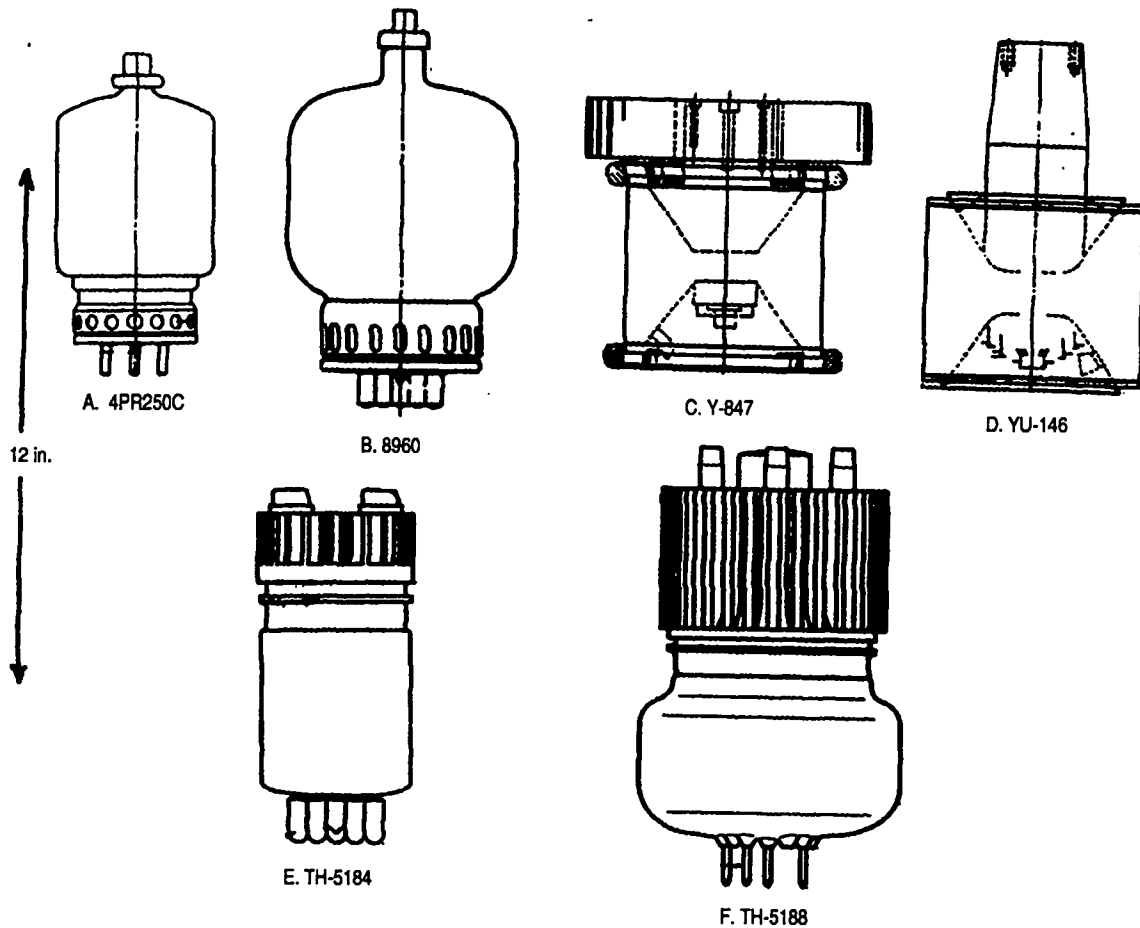


Figure 11-12. Tube types well suited for modulating-anode pulser service.

levels of vibration and shock. Unlike the previous tubes, which were much more mature, it has a unipotential, oxide-coated, indirectly heated cathode that is designed for short-pulse (20- $\mu$ s) service. Its peak-pulse cathode current is rated at 10 A. The relatively short pulse-duration rating is not a serious limitation in modulating-anode-pulser service because switch-tube conduction is required only during either the rise or fall interval, anyway. Its amplification factor,  $\mu_A$ , is 1300, which gives a pretty good idea of how close the grid is to the cathode surface in relation to the cathode-anode spacing. This geometry not only contributes to the dc anode-voltage hold-off rating of 150 kV but to a very short grid base as well (-100 V grid-cathode for plate current cut-off at 150-kV anode voltage). The triode is intended for use in oil-insulated applications, and its anode can dissipate 2000 W when an external radiator is bolted on. (The radiator is shown in the figure.)

#### 11.3.4 YU-146 tetrode

The tube shown as D in Fig. 11-12 is another member of the growing family of modern ceramic-metal, high-voltage switch tubes, except that it is a tetrode with planar geometry. Sharing the ruggedness of the YU-847 triode, the YU-146 is capable of sustaining 60-G shock and 10-G vibration. It is rated for 175-kVdc anode hold-off voltage when oil-immersed with proper corona shielding (not shown in the figure). Its peak-pulse cathode current, from its unipotential, dis-

penser-type cathode, is rated at 20 A for 11- $\mu$ s-duration pulses. Its amplification factors,  $\mu_a$  and  $\mu_{sg}$ , are approximately 2000 and 150, respectively, and its transconductance, which is related to perveance, is 0.15 mho ( $\Delta I_p/\Delta V_G$ ). The anode dissipation is dependent upon its immersion medium, tube orientation, and whether convection is forced or natural. With forced oil convection and horizontal mounting, dissipation can be as high as 10,000 W.

### 11.3.5 TH-5184 tetrode

The TH-5184 tetrode (E) is a tube designed for use in pulsed x-ray equipment. Its anode-voltage hold-off is rated at 85 kV and anode dissipation at 1000 W when immersed in oil. These parameters also make it a serious candidate for modulating-anode-pulser service. Its design is more conventional. It is a glass-envelope tube with a thoriated-tungsten cathode capable of peak-pulse cathode current of 5 A. Also more conventional are its amplification factors, with a  $\mu_A$  of approximately 160 and  $\mu_{sg}$  of approximately 6. Its transconductance is 0.01 mho, which is small compared with the much higher value for the more modern planar-geometry YU-146 tetrode.

### 11.3.3 TH-5188 tetrode

The tetrode illustrated as "F" in Fig. 11-12 is the largest—electrically and physically—and most recent member of this tube family. The TH-5188 is rated to 120-kV anode-voltage hold-off and up to 10,000 W of anode dissipation when operated in oil. Its larger thoriated-tungsten cathode is rated for peak-pulse cathode current of 10 A. Its amplification factors are approximately 500 for  $\mu_A$  and approximately 8 for  $\mu_{SG}$ . Its transconductance is 0.02 mho.

## 11.4 Some representative modulating- anode pulser designs

### 11.4.1 The BMEWS dual-klystron modulator

The dual-klystron transmitters designed for use in the Ballistic Missile Early Warning System (BMEWS) used the very first radar-type modulating-anode klystron, the X-626, which operated in the UHF band. It was rated at a peak RF power output of 1.25 MW when operated with 2-ms-duration pulses at a 30 pps repetition rate, with continuously applied cathode voltage of up to 120 kVdc, and with modulating-anode voltage swing of about 2/3 of the cathode voltage. The physical arrangement of the dual klystrons and their floating-deck modulating-anode pulser, which may very well have been the first of its type, is shown in Fig. 11-13.

The transmitter was designed by Continental Electronics, then and now a designer and manufacturer of high-power radio-broadcast transmitters. It was built at a time when fiber-optic links were unheard of. It should not be surprising to learn that the then-very-daunting problem of small-signal coupling to the two floating electronic decks, especially the "on" deck, was solved by radio broadcast. Each of the two pulse decks, "on" and "off," had its own receiving loop antenna. Between them was a third loop antenna, the transmitting antenna. For the duration of each desired transmitter output pulse, a burst of a pulse-modulated, 5-MHz, radio-frequency signal was fed into the transmitting loop from a not-inconsiderable RF source. The signal was simultaneously picked up by the

two receiving loops and rectified within the two decks to produce a gating signal to the high-voltage switch tubes. (This topology is similar to the one shown in Fig. 11-3.) The gate turned off the "off" switch tube and turned on the "on" switch tube. The anode of the "on" switch tube was maintained at a positive voltage (with respect to klystron cathode voltage) of approximately two-thirds of its cathode voltage by means of a fixed resistive voltage divider and shunt energy-storage capacitor. The resistive/capacitive voltage divider supplanted the function of the variable power supply shown in Fig. 11-3. It was possible to do this because the repetition rate (30 pps) was invariant and, therefore, the average modulator current was constant.

This class of transmitter, which became populated by ever-more-modern klystrons over its long life span, has only recently been replaced by highly modular, solid-state phased-array radar systems of the Pave Paws type. The decommissioned klystron transmitters are usually snapped up eagerly by other users, by the way.

#### 11.4.2 The Millstone Hill radar transmitters

One such eager user of BMEWS-class transmitters was the Millstone Hill Radar Facility at Westford, Mass., which employs three of the dual-klystron transmitters. Two use UHF klystrons. The third transmitter uses X-780 L-band

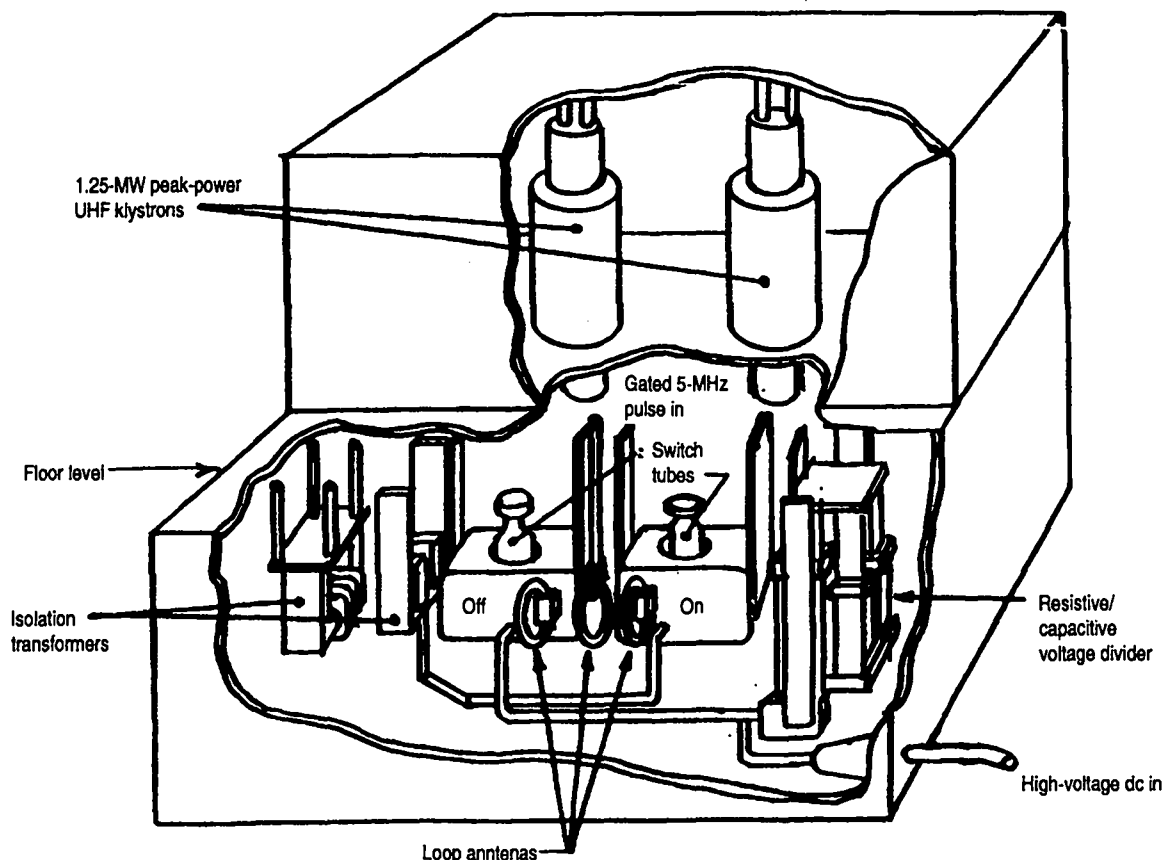


Figure 11-13. An early (if not the first) modulating-anode pulser.

klystrons, which produce 2.5 MW peak power each. Of the UHF transmitters, the first started with the ancient X-626 external-cavity klystrons, which were later replaced by the L-3403. At present, one of the two transmitters has been upgraded to the high-efficiency version of the L-5773, which produces almost as much power from the two klystrons as was previously obtained from all four combined.

Originally, the modulators for these transmitters were the BMEWS type. They had virtually no repetition-rate agility or amplitude variability, and their rise-and-fall times were excessively long for the radar experiments that were later

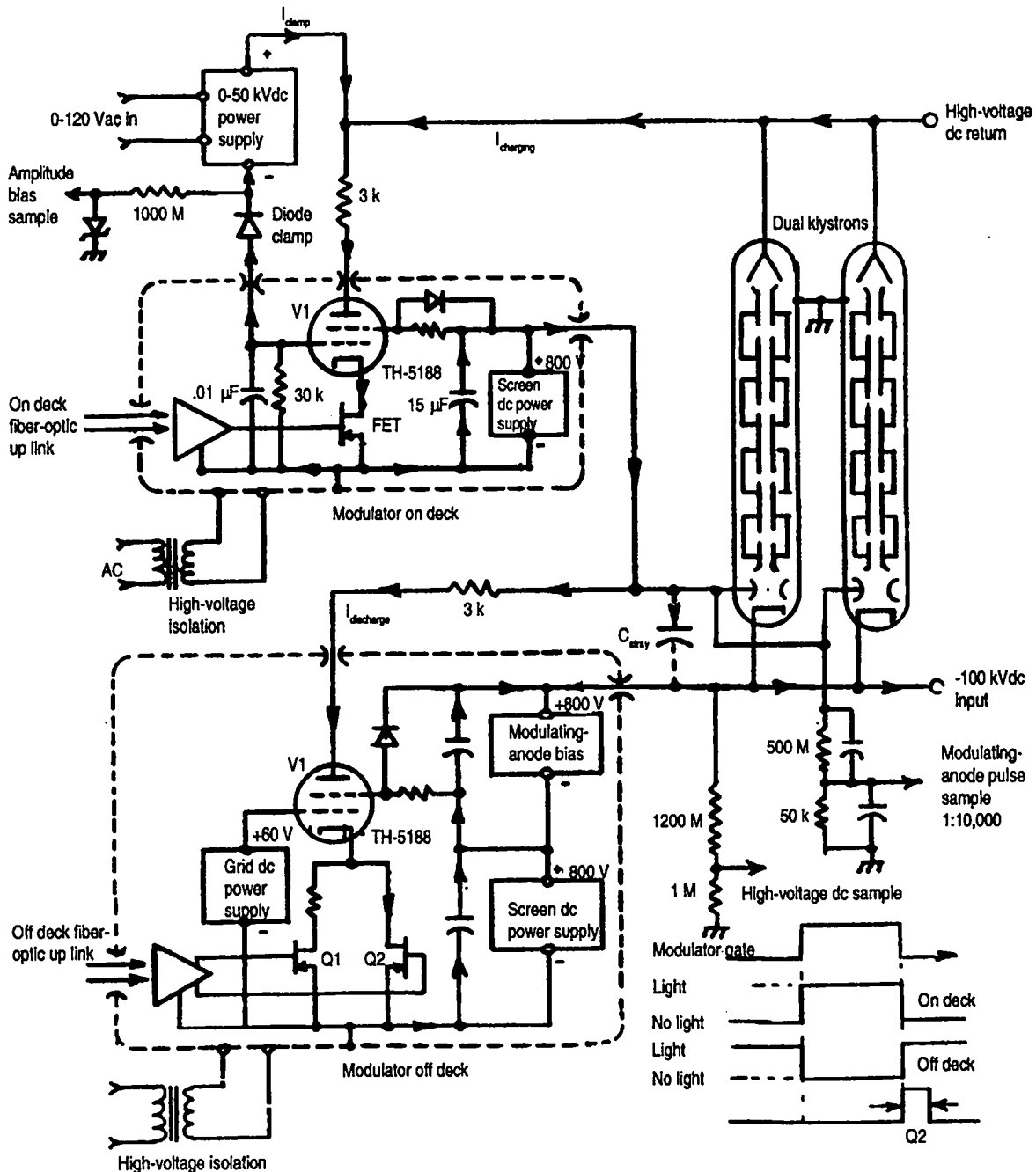


Figure 11-14. The modulating-anode pulser for the Millstone Hill dual-klystron radar transmitter.

contemplated. For these reasons they were eventually modified to the type shown schematically in Fig. 11-14. This design represents a classic embodiment of the active-pull-up, active-pull-down, grid-catcher amplitude-control topology using TH-5188 tetrode switch tubes. Even though the basics of this arrangement have been previously discussed, there are a few changes worth noting.

The first is the use of an external resistance in series with each anode of the two switch tubes. This resistance serves dual purposes. It is small enough (3 kohms each) so that it does not significantly reduce peak-pulse switch-tube anode current, which means that it is not large when compared with the incremental anode resistance of the tubes. It will, nevertheless, share the total power dissipation incurred in repetitively charging and discharging the load capacitance (some 600 pF) with the switch-tube anodes. More importantly, it limits the "shoot-through" fault current that may result from simultaneous arcs in the "on" switch tube and in the klystron between the modulating anode and cathode, or simultaneous arcs in the "on" and "off" switch tubes. Neither coincidence is impossible.

Note also that the output from the "on" deck and the return connection from the "off" deck are diode-coupled from the screen grids of the switch tubes rather than from the deck connections. This is because an internal arc in either switch tube will be from anode to screen grid. The fault current, therefore, is diverted to the external circuitry by way of the diodes, thus minimizing the likelihood of arc-through to control grid and then cathode, an event that could greatly jeopardize the switching transistors. For the "off" deck, this approach provides the additional advantage that the screen-grid power supply biases the source electrodes of the switching transistors negative (with respect to the klystron cathode voltage). These transistors are in the conducting state during the interpulse interval, turning on the "off" switch tube. Once saturation conduction has been achieved, its anode is therefore also negative (with respect to the klystron cathode voltage), providing negative modulating-anode bias for the klystrons during the interpulse interval. In this circuit there is an additional bias power supply. (Actually, the screen voltage is taken from the midpoint of a single power supply.) The price for double duty from the screen supplies is that they must be rated for the entire average current of the modulator rather than just for the average screen-grid current.

The two switching transistors in the cathode circuit of the "off" tube, *Q1* and *Q2*, provide two states of conduction for the "off" switch tube. At the beginning of the fall time of each pulse, both transistors are pulsed into conduction. Transistor *Q2*, which has no resistor in its drain circuit, conducts the full discharge current of the "off" deck, rapidly terminating the pulse. After a time delay of slightly longer than the normal fall time, *Q2* is gated off. Transistor *Q1*, however, continues to conduct. The resistor in its drain circuit is selected to cathode-bias the switch tube so that plate current is a few milliamperes but the screen-grid current is negligible. The tiny bleed current is usually adequate to handle leakage current that may flow across the inner surfaces of the ceramic insulators between the modulating anodes and bodies of the klystrons. (This leakage is due to barium-based deposits from the cathode.) Without a current sink with low voltage drop, which the barely conducting switch tube provides, the leakage

current could pull up the klystron modulating anodes sufficiently to cause low-level, but continuous, beam current, which can be extremely injurious to the klystrons. (Actually, large klystrons with oxide-coated cathodes are less likely to exhibit ceramic-bushing-leakage current than some of the more modern, high-power travelling-wave tubes that have dispenser-type cathodes.)

The new modulators at Millstone Hill were successful. They have permitted transmitter operation at pulse repetition rates up to 1000 pps with pulse rise-and-fall intervals on the order of 10  $\mu$ s. And they have allowed the use of complicated waveforms.

#### 11.4.3 *Dual-klystron modulating-anode pulser for particle-accelerator RF source*

Not all modulating-anode pulsers are built for dual-klystron transmitters, but the example shown in Fig. 11-15 is another one. In this case, the microwave amplifier tubes are 1.25-MW-peak-power klystrons, operating at 850-MHz and a pulse-repletion rate of 10 Hz. They require approximately 90 kVdc for their cathode voltage and are used as the input to drift-tube linear-accelerator cavities. What is unique about this modulator, which has an active-pull-up, passive-pull-down topology, is that it has a two-stage grid-catcher circuit for its pull-up pulse deck.

The high-voltage electronic switch is an L-5012 beam-switch tube that is used at only a fraction of its collector-current capability. Resistive pull-down is tolerable because the pulse duration is long, 2 ms, and the maximum accelerator duty factor is only 2%. Furthermore, this application of RF power is unlike a monostatic radar-system transmitter, where a klystron's beam-induced receiver noise following the transmitter pulse can limit the system's minimum range. Such noise is not a concern in an RF source for a particle accelerator. The 100-kohm pull-down resistor, *R1*, produces a sufficient fall time.

The modulating anode of the L-5012, *V2*, is pulsed to approximately 2.5 kV positive (with respect to its cathode) by a bootstrap-connected driver stage (a bootstrap within a bootstrap) comprising a 4PR125 tetrode, *V1*, and a cascode-connected FET switch, *Q1*. The return for *Q1* and the optically coupled low-level gate-drive circuit is the modulating-anode of *V2*. The grid-catcher diode *CR1* is connected to the grid of *V1*. When the optically coupled "on" gate is received, *Q1* is turned on. This transistor pulls the cathode of *V1* low, pulsing it into a zero-bias conduction state. This action connects the positive terminal of the 2.5-kVdc power supply to the modulating anode of *V2*, pulsing the L-5012 into conduction, which commences charging the load capacitance and building up current in *R1*. This build-up continues until the modulator output voltage is approximately 2.5-kV more negative than the voltage across *C1*, which is the storage capacitor for the voltage-divider-type amplitude control (as in Fig. 11-6). When this point is reached, *CR1* begins to be forward-biased and the shut-off process of *V1* commences, clamping the modulator output voltage.

When the low-level gate signal ends, drive is removed from the modulating anode of *V2* and the trailing-edge commences, the fall time of which is primarily determined by the value of *R1*. The value of the resistance shunting the *V2* modulating anode to its cathode circuit can also affect fall time because it is the sink for the "Miller" capacitance current that flows between the *V2* collector and

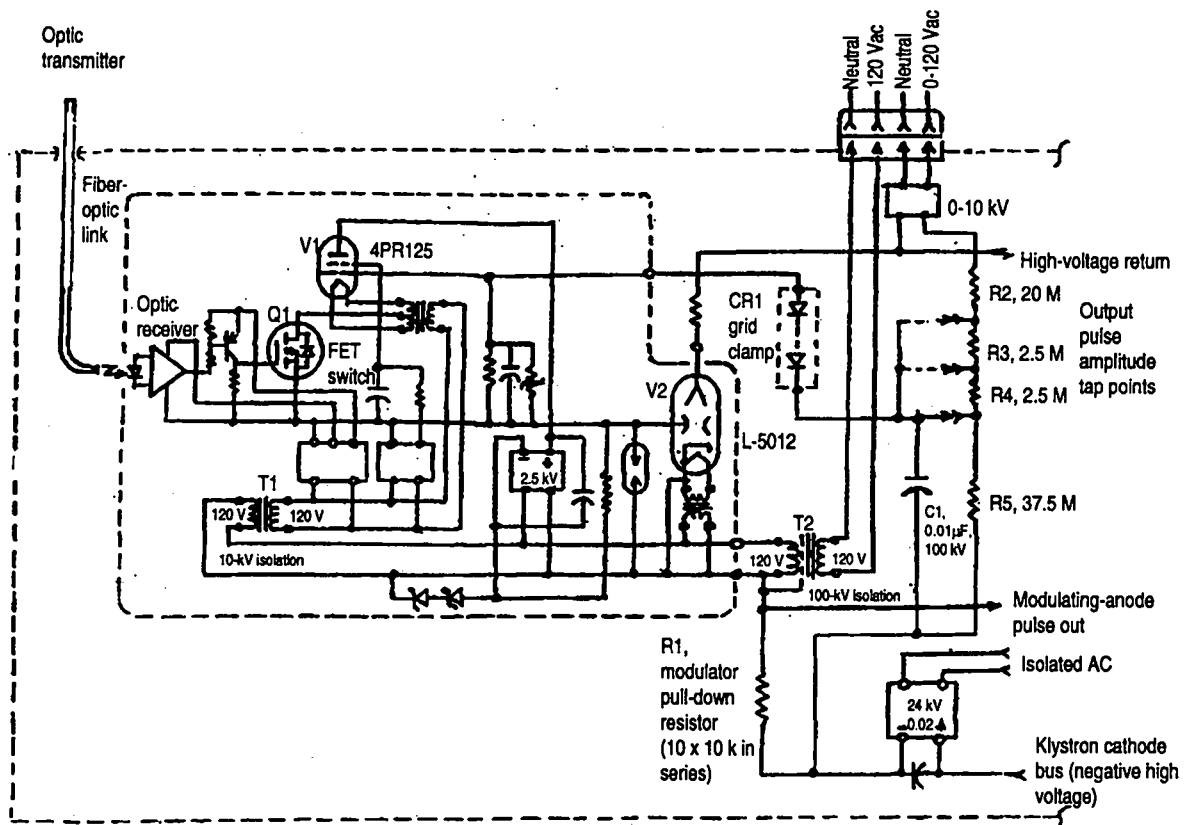


Figure 11-15. Simplified schematic diagram of dual-klystron modulating-anode pulser for particle-accelerator high-power RF system.

modulating anode.

Exploded views of the physical arrangement of the dual-klystron RF station are shown in Fig. 11-16. The self-capacitance of the modulator pulse deck is quite high because the dimensions of the deck are not only relatively large, 10 in. x 20 in. x 17 in., but the deck is immersed in a tank of synthetic dielectric oil having a relative permittivity of 3.2. If we calculate the self-capacitance of the deck in air using the methods described in Section 11.2, a value of approximately 120 pF is obtained. A measurement of the total capacitance from modulating-anode bus to ground, with no oil in the tank, gives a value of approximately 230 pF. This includes the modulating-anode capacitance of the two klystrons (a total of about 100 pF) and the capacitance of the power isolation transformer for the pulse deck (about 11-15 pF). All of the capacitance, except that inside the vacuum envelopes of the klystrons, will be multiplied by a factor of 3.2 when the tank is filled with dielectric fluid, bringing the total capacitance to about 500-600 pF. The discharge time-constant of the passive pull-down is, therefore, approximately 50-60  $\mu$ s. But the measured trailing-edge discharge time-constant operating in oil is 80  $\mu$ s.

This additional time is introduced by the "Miller-effect" time-constant of the switch-tube driver. These two time-constants, which are isolated from one another but are cumulative, are added together as the root of the sum of the squares of the individual time-constants. The resulting calculation of the driver-stage

discharge time-constant indicates it is approximately the same as the external pull-down constant. (If the time constants were exactly equal, they would produce a result that is the square root of 2 multiplied by each individual time-constant.)

A note of caution: measuring low-level signals within pulse decks and high-voltage, or "hot," decks can be lethal. To make such measurements requires that an oscilloscope or meter be "floated" so that its signal common is at deck potential. Failure to observe this rule can have a tragic outcome. (At least one engineer and one technician have been killed as a result of such carelessness. The temptation to reach out and make adjustments to the test equipment is often irresistible—but never habit forming.)

#### 11.4.4 The modulating-anode pulsers for the MAR-1 radar system

The Multi-function Array Radar 1, or MAR-1, was developed during the mid-1960s. It was an experimental, phased-array (PA) radar designed to be part of the Safeguard anti-ballistic-missile defense system, which was the first system to time-sequentially accomplish the functions of target acquisition, tracking, and discrimination within a single pulse-repetition interval. It achieved this by using the electronic agility and broad bandwidth of true time-delay steering, which governed the separate transmitting and receiving antenna arrays. This radar was the test bed that led to powerful PA systems such as Cobra-Dane, Cobra-Judy, the Perimeter-Acquisition Radar, and even the SPY-1 radar of the Aegis weapons system. Most of these systems are still operational. But unlike its successors, MAR-1 was purely experimental. It had no long-term operational mission. (Part of the experiment was to see if it could be operated by Army enlisted personnel.)

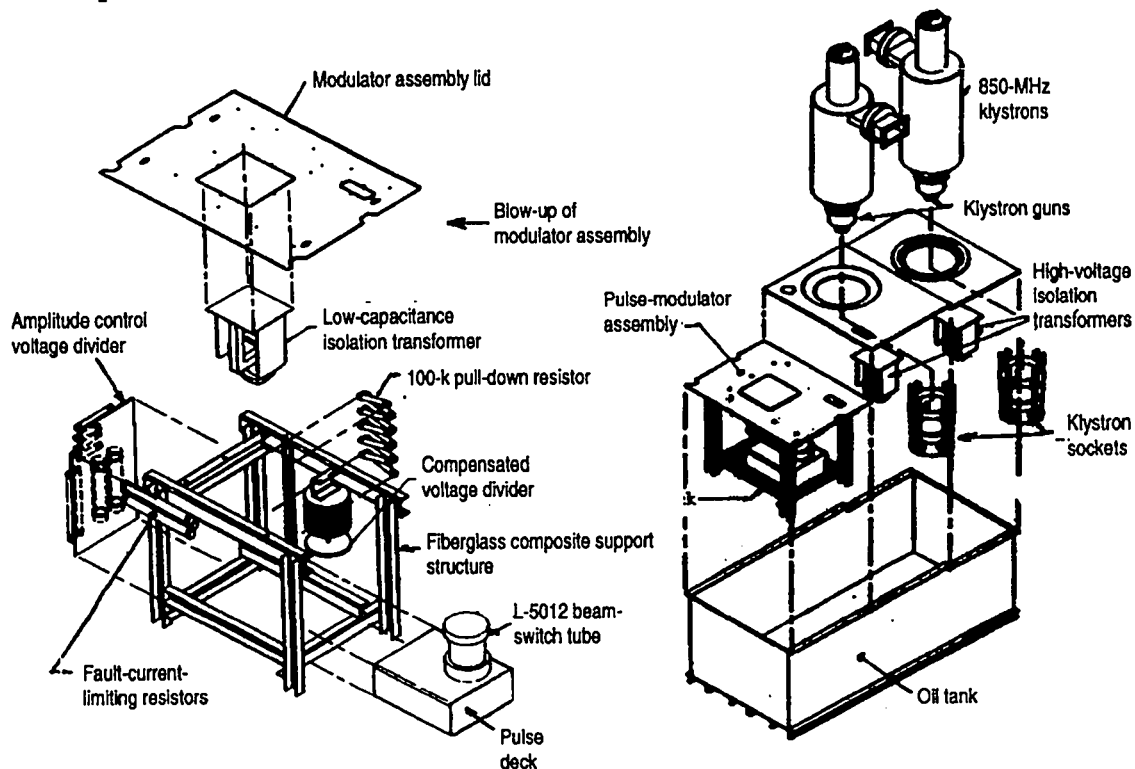


Figure 11-16. Physical arrangement of 850-MHz dual-klystron RF station.

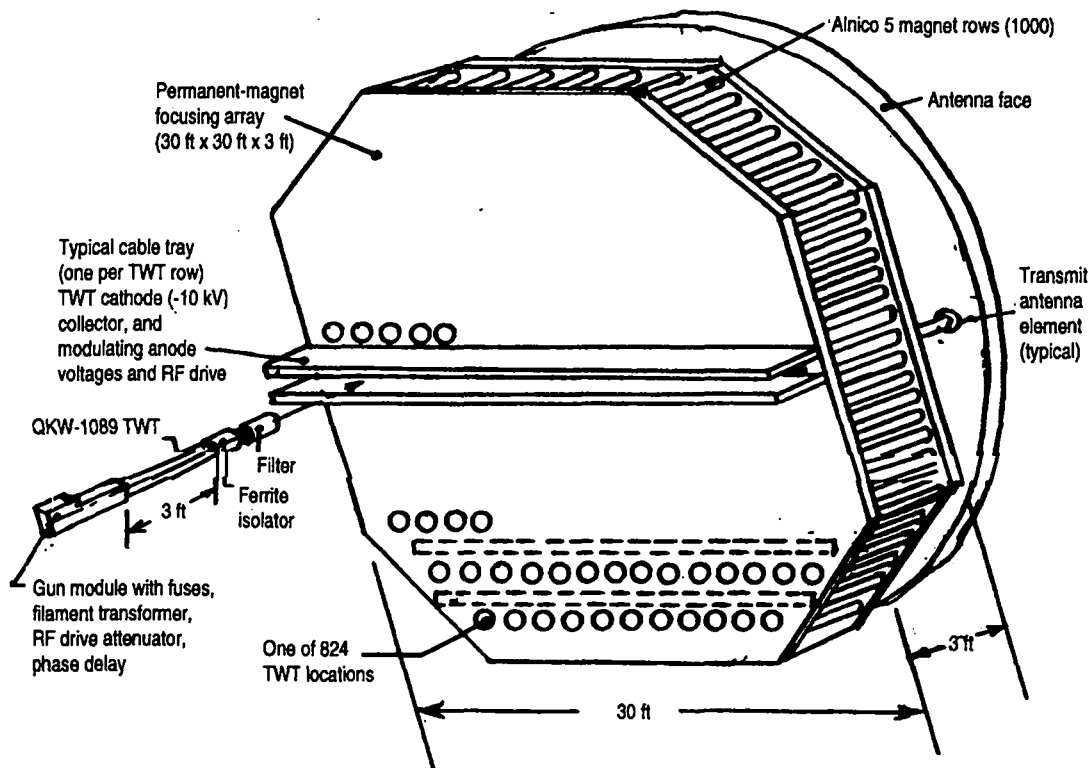


Figure 11-17. Simplified representation of the MAR-1 transmitter-array face.

It could.)

Its transmitting-array antenna, which used a total of 824 TWT RF power amplifiers, was electronically steered by the switching of incremental time delays that took the form of transmission-line segments, which were graded in delay time in accordance with a binary progression in the low-level input paths of each of the TWT PAs. A feature of this transmitter, shared by none other, was the means of focusing the 824 TWTs, which is illustrated in Fig. 11-17. Whereas tubes of this type, which have 5 kW of peak-power output at L-band, are routinely focused by means of periodic permanent-magnet stacks or solenoidal electromagnets that surround their 3-ft-long interaction regions, none had ever been focused by a uniform-field permanent magnet system. The reason for this is the field produced by a permanent magnet for a tube that is long and skinny is inefficient. Most of the magnetic energy will be located in the fringing fields.

If, however, one approaches the focusing of all 824 TWTs as an ensemble, what can result is what is shown in Fig. 11-17: a single, monolithic, permanent magnet whose iron pole-pieces are 30 ft on a side but separated by only 3 ft. The form factor of the design has gone from long and skinny to short and fat, and for that reason the magnetic energy lost to fringing fields becomes a trivial portion of the whole. Just such a magnet was built and energized by a total of 1000 permanent-magnet rods made of Alnico 5. The individual TWTs, for their part, had dislike iron field-straighteners arrayed along their lengths to short-circuit transverse magnetic-field components along their beam axes. The combination worked.

Although one of the candidate TWTs had a gridded-electron gun, it was

Group	TWT count	Group	TWT count
A	41	K	41
B	41	L	41
C	41	M	41
D	41	N	41
E	41	O	41
F	41	P	41
G	41	Q	42
H	41	R	41
I	41	S	42
J	40	T	40

Table 11-2. Grouping of the 824 TWTs for the MAR-1 transmitter.

decided that operation of multiple tubes from a single bus would be more feasible if the tubes had full-voltage modulating anodes instead. For the purposes of dc and modulation-pulse inputs, the 824 TWTs, were divided into 20 separate groups, A through T, as shown in Table 11-2. Each group had as many as 42 TWTs as loads, and each group had its own dc power supply, energy-storage capacitor bank, operating controls, and, of course, modulating-anode pulser. Unlike most such applications, these TWTs were physically remote from their modulating-anode pulsers and were interconnected by high-voltage coaxial pulse cables having significant distributed capacitance (at a rate of typically 30 pF/ft). Furthermore, the TWTs associated with a given pulse modulator were not placed in adjacent rows; the original design called for three separate pulse cables from each modulator to the feed ends of three cable trays. (Before the transmitter became operational, however, this design was modified. A single cable from each modu-

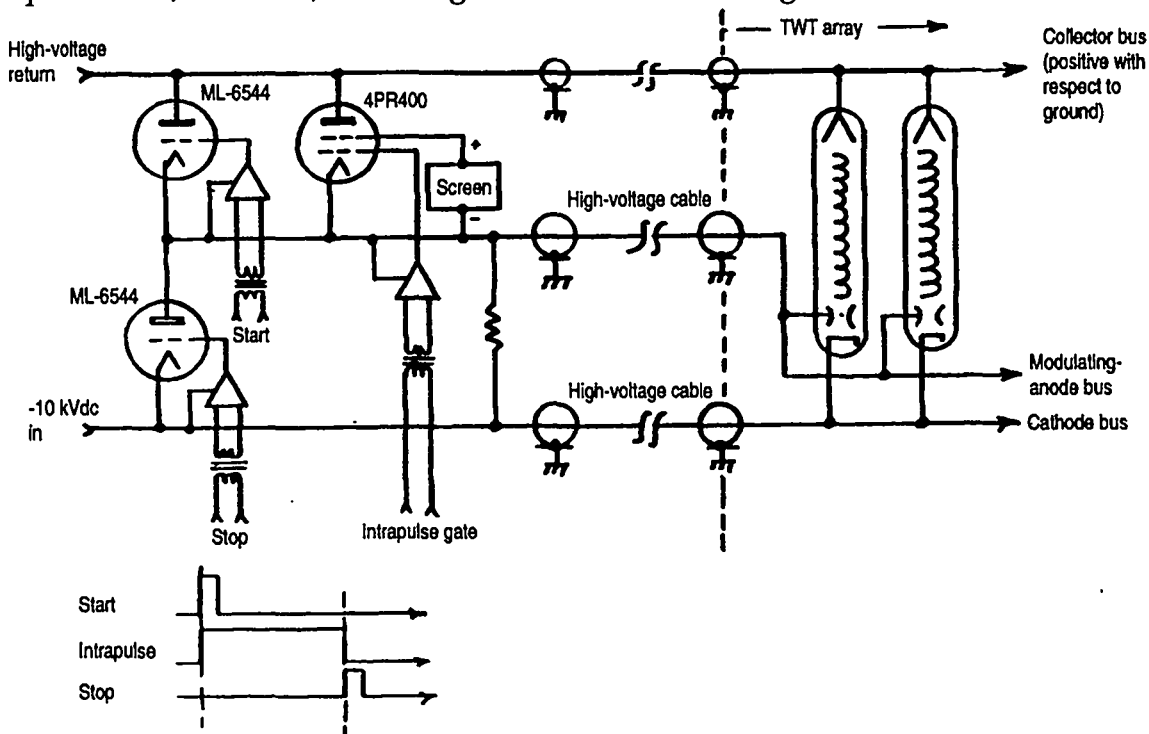


Figure 11-18. Simplified schematic diagram of one of twenty MAR-1 transmitter pulse modulators.

lator was used. This cable, in turn, fed into an intermediate junction box at the periphery of the magnet assembly, from which shorter jumper cables split out to the individual cable trays. This also solved the problem of a 2-MHz oscillation that was superimposed on the modulating-anode output voltage.)

The pulse modulators themselves, shown in Fig. 11-18, had active pull-up and pull-down provided by two ML-6544 triodes, which are more commonly encountered in cathode pulsers. These tubes conducted only during the rise-and-fall intervals of the output pulse, charging and discharging the load capacitance and making full use of the short-pulse, high current available from their oxide-type cathodes. A third switch tube, a 4PR400, had a long-pulse thoriated-tungsten cathode. It is shown shunting the pull-up tube. Its function was to supply the significant intrapulse modulating-anode interception current for as many as 42 parallel TWTs. Even if individual TWT modulating-anode current was 0.1% of cathode current, the total current for 42 tubes is 4.2% of total cathode current, an amount that cannot be ignored.

The start, stop, and intrapulse low-level gate signals were coupled to the switch-tube drive circuits by means of special pulse transformers that had a high degree of electrostatic isolation. Even so, the common-mode-rejection problem was formidable, especially for the pull-up deck. And this problem was further aggravated by the use of SCRs to discharge small PFNs, which functioned as the grid-drive-circuit active elements. The SCR gate circuits proved to be far too sensitive for such an application, although they were eventually made to work.

#### *11.4.5 The long-range imaging radar transmitter modulating-anode pulsers*

Located atop Haystack Hill (the next hill north of Millstone Hill near Westford, Mass.), the long-range imaging radar (LRIR) represents a category of radars known as inverse synthetic-aperture imaging radars. These radars use target motion instead of antenna motion to generate the synthetic antenna aperture. The LRIR operates in the X-band and has the range resolution that 1-GHz instantaneous bandwidth can provide (9.5-11.5 GHz). (The processed-signal equivalent of a transmitted pulse from LRIR has duration of 1 ns, which means it occupies approximately 1 ft of radar range extent.) And it has the cross-range resolution that the beam width of a 120-ft-diameter parabolic reflector can provide. Its transmitted power and receiver noise-floor characteristics are such that it can produce radar images of objects in geo-synchronous orbit 22,000 miles away.

The transmitter's RF high-power amplifier, which is shown in Fig. 11-19, comprises four VTX-5681 coupled-cavity TWTs. These tubes are rated at 100 kW of peak power and 30 kW of average power. (Originally, the tubes were supposed to be capable of 50 kW average power, but this requirement was downgraded to 30 kW as part of a cost-reduction modification.) Worthy of note is the high-power waveguide system, which was constructed in a special waveguide size, WR-102 (0.102-in. internal spacing between narrow walls instead of the 0.09-in. spacing for the standard WR-90 waveguide for this frequency band). WR-102 is the largest waveguide that can be used without incurring higher-order mode problems. The input to the high-efficiency, multi-mode tracking-antenna feed is in the form of eight equi-amplitude, equi-phase signals, which presumably could have been obtained by splitting the outputs of the four TWTs into two channels



each. Doing so, however, would not have yielded eight channels of sufficient amplitude and phase identicalness over the entire 1-GHz bandwidth. (The differences in phase- and amplitude-transfer characteristics between individual TWTs are too great.)

To overcome this problem without combining the total output power in a single waveguide segment, five stages, or ranks, of combiners are used. The output of each pair of tubes is combined in the first rank of 3-dB hybrid combiners and then immediately split into two channels again in the second rank of 3-dB hybrids, which produces twice the power of a single TWT in each of two waveguide segments. These signals are then cross-combined, with one channel from each original pair of tubes combining with the remaining channel from the other pair in the third rank of hybrids, again producing twice the power of a single TWT in each of two waveguide segments. Now the composite signals in the two segments are identical to the extent that the passive waveguide components are identical. And at each frequency throughout the pass band, the composite signals are the average of the characteristics of the four TWTs. These signals are finally split into the requisite eight channels by the next two ranks of hybrids. Needless to say, all the high-power waveguides are water-cooled. The stainless-steel flanges compress soft-copper gaskets at each waveguide junction. The number of such junctions is minimized because the entire splitter/cross-combiner assembly is integrated.

The TWT electron guns, which operate at cathode voltage of just below 50 kVdc, have nearly full-voltage modulating-anode beam-current control to gate their 11-A peak-beam current. The modulating-anode pulser, as shown, is of the grid-catcher type. It has an active pull-up and pull-down and uses the type 8960 glass-envelope tetrode, which has adequate anode dissipation to permit repetition rates up to 2000 pps at the shortest pulse durations. The maximum pulse duration is 50 ms (50,000  $\mu$ s), which represents a high-stress condition for the TWTs but not for the modulator. The entire front end of the transmitter is air-insulated and, along with the receiver preamplifiers and downconverters, is mounted in an 8-ft x 8-ft x 12-ft enclosure that weighs 7000 lb. The feed horn, which is affixed to one end of the enclosure, is hoisted to the rear of the 120-ft parabolic reflector and slid forward so that the feed protrudes through a hole in the center of the main reflector and illuminates a subreflector that is part of the Cassegrain optics.

When originally put into service, the modulator was unique in that its low-level signal-coupling to the "on" and "off" decks was accomplished by means of capacitively coupled, balanced RF transmission lines. The inputs to them were in the form of pulse-modulated bursts of 11-MHz RF. The modulation envelopes corresponded to the desired modulator pulse-voltage output timing. (In effect, this was an update of the original BMEWS transmitter RF signal-coupling.) The balanced nature of the signal-coupling and the high ratio of the 11-MHz signal to the highest frequency component in the output pulse provided adequate common-mode signal rejection, even though the RF source was a computer-clock integrated circuit (IC). This IC, unlike the powerful 5-MHz transmitter used in the BMEWS-type transmitter, interfered with nothing else in the system. The capacitance of the signal link to the "on" deck and its voltage-equalizing shunt

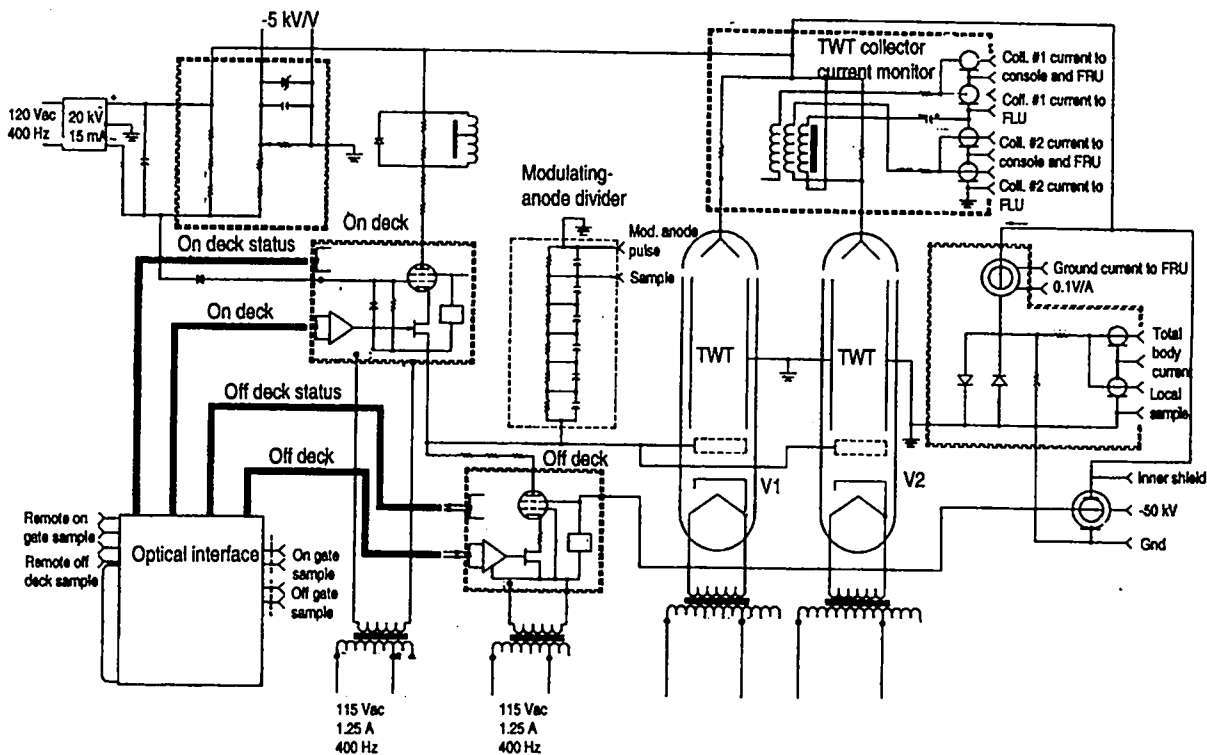


Figure 11-20. Simplified schematic diagram of modulating-anode pulser and dual-TWT high-power amplifiers of HAX transmitter.

resistance also doubled as part of the frequency-compensated voltage divider, which provided a direct-coupled sample of the modulator-output voltage. This original signal-coupling method has since been supplanted by modern fiber-optic signal links.

#### 11.4.5 The modulating-anode pulser for the Haystack Auxiliary Radar (HAX)

Nearing completion in early 1993 is the Haystack Auxiliary Radar (HAX), which has its own dedicated, full-time 40-ft Cassegrain-optics antenna. (The LRIR described above must time-share its antenna with a number of box-mounted, physically interchangeable radio-telescope receiving systems.) HAX will have twice the bandwidth of the LRIR, 2 GHz, and operate in the  $K_U$  band. Its high-power RF amplifier consists of a pair of state-of-the-art coupled-cavity VTU-5692-type TWTs, which have re-entrant, double-staggered-ladder RF circuits. These TWTs are capable of as much as 60 kW peak-power output at 30% duty factor.

Along with the multi-channel low-noise receiver components, the entire front end of the transmitter, shown in Fig. 11-20, must share a fixed equipment compartment mounted behind the parabolic reflector. This compartment is quite a bit smaller than the RF box for the LRIR system. Despite the size limitation, however, the performance requirements for the modulating-anode pulser are very nearly the same as those for the LRIR transmitter modulator. The topology used is the same—active pull-up and pull-down, grid-catcher amplitude control—but everything has to be smaller.

The switch tube chosen is the highly capable 4PR250C. But at the maximum PRF of 2000 pps, its 250-W anode-dissipation rating is not enough. To help physically and electrically, the dimensions of the modulator decks are minimized, thus reducing the self-capacitance component of the modulator load capacitance and allowing the decks to fit in the available space. (This solution was facilitated by using 400-Hz primary power from a remotely located electronic static inverter.) Using a 400-Hz power supply allows the designers to use much smaller magnetic components, especially the filament transformers. Using smaller components permits deck dimensions of 6 in. on a side—just large enough for the tube socket. The other key enclosure-mounted components, including the low-capacitance power-isolation transformer for the “on” deck, the high-voltage isolation transformers for the “off” deck, and the two TWT filaments, can be reduced in size as well. (See Fig. 11-21.) To share the power dissipation with the switch tubes, current-limiting series resistance is used in the anode circuits of both switch tubes. The resistance in series with the “on” tube is great enough to noticeably affect the rise time of the output pulse. Half of the resistance, therefore, is shunted by an inductor that “shunt-peaks” the response, giving a rise time of less than 10  $\mu$ s.

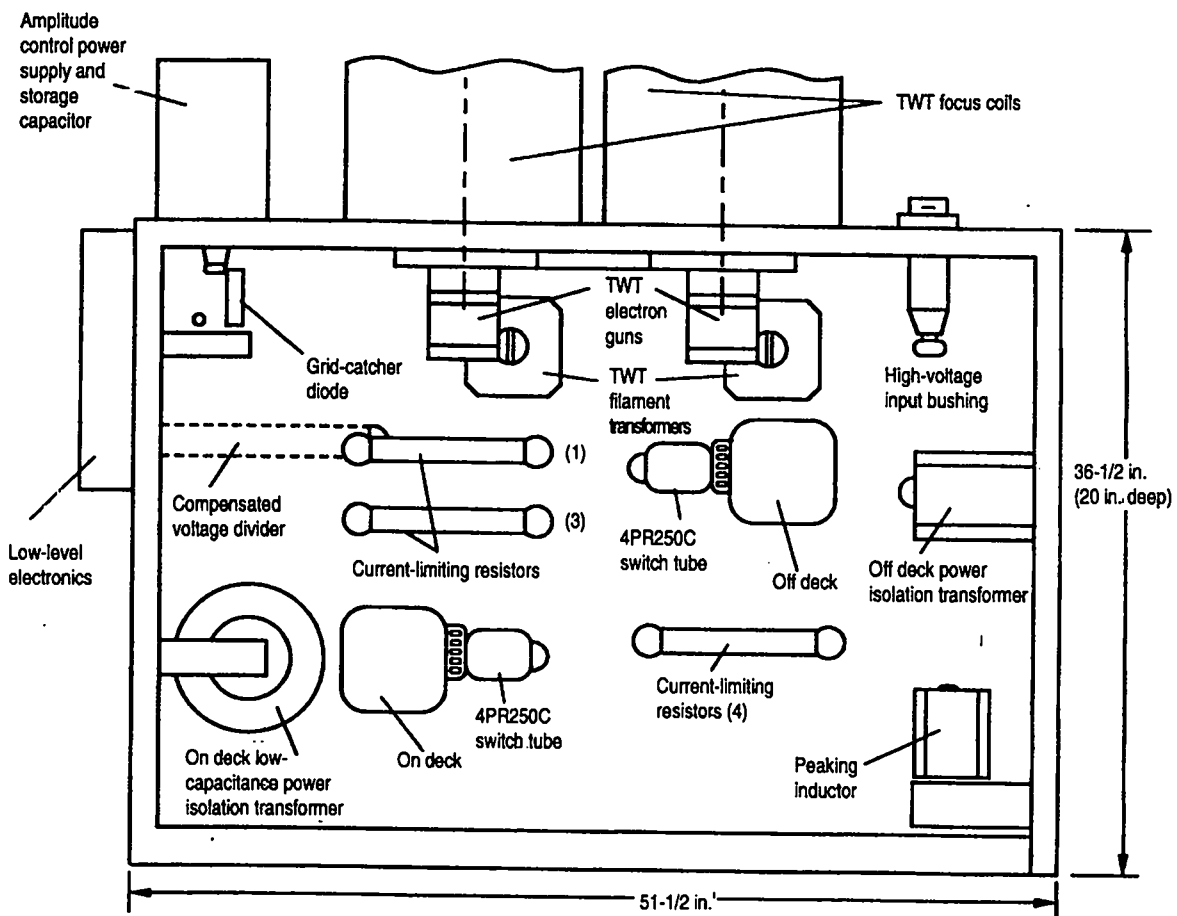


Figure 11-21. Arrangement of components and subassemblies of HAX transmitter pulser.